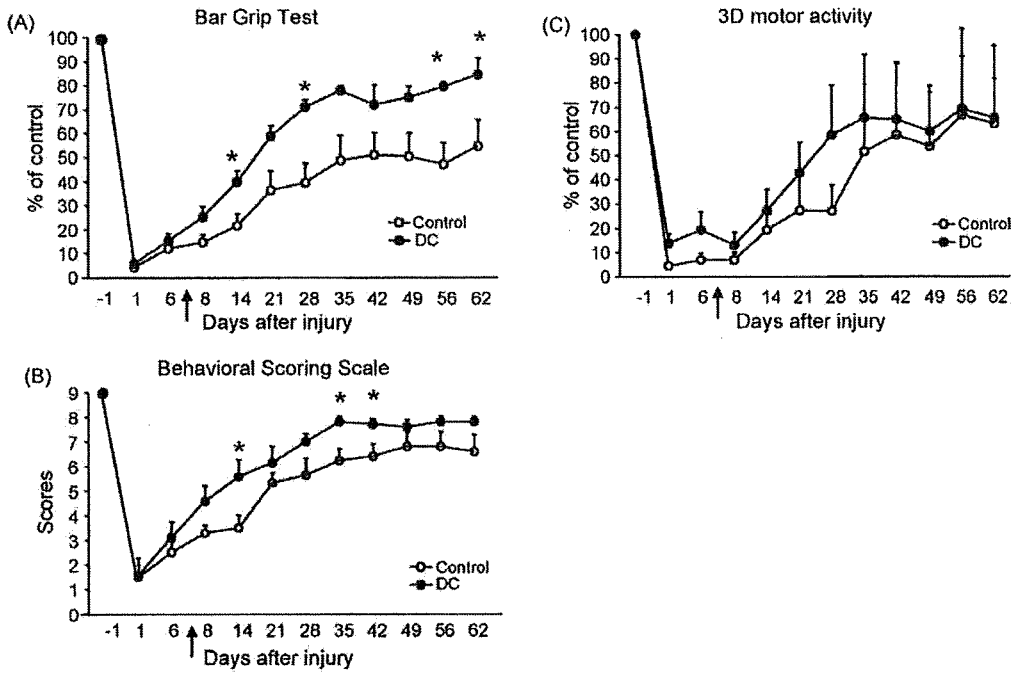

Fig. 6. Behavioral analyses of SCI-CMs after DC-transplantation. (A) Bar grip test. The time course of the bar grip power in control and DCs-treated CMs. Each value indicates the percentage of bar grip power before injury (DC-treatment, $n = 5$; control, $n = 5$). (B) Behavioral scoring scale. The scores (1–9 points) was given for each representative motion, as described in Section 2 (DC-treatment, $n = 5$; control, $n = 5$). (C) 3D measurements of spontaneous motor activity. The value indicates the percentage of spontaneous motor activity before injury (DC-treatment, $n = 5$; control, $n = 5$). Arrow indicates the day of DC-treatment. $^*P < 0.05$, Mann–Whitney U-test.

progenitors, leading to the enhancement of remyelination. Future studies are required to analyze endogenous NSPCs in CM *in vivo*.

Several reports of immune-cell-based therapy have described the treatment of SCI. Activated microglia have been shown to secrete neurotrophins *in vitro* (Elkabes et al., 1996; Miwa et al., 1997; Nakajima et al., 2001) and *in vivo* (Batchelor et al., 1999; Bouhy et al., 2006). These neurotrophins promote neuronal survival and axonal regeneration in SCI (Prewitt et al., 1997; Rabchevsky and Streit, 1997). Recently, skin-derived macrophages (Knoller et al., 2005) and bone marrow cells with GM-CSF (Yoon et al., 2007) showed beneficial effects on SCI in clinical studies. One of advantages of DC therapy is that autologous transplantation can be performed; DCs are generated from monocytes in peripheral blood of patients within a week (Babatz et al., 2003). The therapeutic time window including the timing of such treatment is important in SCI therapy. Many studies suggest that delayed administration (1–2 weeks after SCI) of cells is suitable for the treatment of SCI (Ogawa et al., 2002; Okano, 2002; Okada et al., 2005; Bouhy et al., 2006; Iarikov et al., 2007; Iwanami et al., 2005a), because inflammatory reactions in the acute phase may inhibit survival of transplanted cells. Considering how easily such cells can be obtained, the timing of the treatment, and the lack of allograft problems, DC are a useful cell type for SCI therapy in humans.

In this study 4–8 $\times$ 10^6 DCs generated from BM cells were transplanted into the spinal cord, although the same number of DCs should be transplanted in each animal. In our previous study, one million cells were implanted into the mouse spinal cord (Mikami et al., 2004). If the same cell number per body weight is used, approximately 10 million cells should be transplanted into each CM. However, it is very difficult to obtain 10 million cells from a donor CM. In clinical studies, various cell numbers of immune cells (4–200 million cells) were transplanted into the human spinal cord (Knoller et al., 2005; Yoon et al., 2007). From human peripheral blood, 100 million DCs can be obtained (Motta et al., 2003). Therefore, we transplanted the maximum cell number of DCs obtained from a donor CM in each experiment. In addition, in the protocol of this study, we performed DC sorting and the surgery for the DC-transplantation on the same day. The number of DCs generated *in vitro* from the same number of BM cells differed among the experiments, since the yield of DCs depended upon individual factors (Ohta et al., 2008). A considerable length of time was required to sort the DCs using FACS because of the small population of CM-DCs in the BM cultures. These technical problems also caused the cell number of DCs used for transplantation to differ among the experiments. In future studies progressing toward clinical application, the cell number of DCs used for transplantation into the spinal cord will need to be optimized.

The safety of DCs for cancer therapy has already been demonstrated in humans. Observations of the general health conditions revealed no apparent differences between control and DC-treated CMs. In this study, we also followed weight changes to monitor health conditions during the experiments. No significant weight loss was observed in CMs after DC-transplantation. Moreover, the spontaneous movements of the DC-treated CMs were always better than those of the control CMs, although the difference was not statistically significant (Fig. 6C). In the histological analyses, no apparent additional damage to the spinal cord was observed after DC-transplantation. Although further safety studies are required to realize clinical applications, these results suggest the safety of administering DCs into spinal cord lesions.

Compared with rodents, CMs have distinct differences in anatomy and functional neural circuits of the spinal cord (Fujiyoshi et al., 2007). Thus, our study in CMs may be important for the preclinical evaluation of DC therapy for human SCI. DC-transplantation showed a neuroprotective effect on SCI, leading to functional recovery in CMs. Taken together, our results suggest that DC therapy has major potential for the treatment of SCI in the clinical setting.

Acknowledgments

This work was supported by grants from the Ministry of Education, Culture, Sports, Science and Technology (MEXT), Japan and a Grant-in-aid for the Global COE program to Keio University from MEXT. We thank Dr. F. Toyota, Dr. H. Ishi, and Y. Tanioka (Central Institute for Experimental Animals) for their technical assistant with the operations and the animal care of CMs. We thank M. Kokubo, T. Muraki, and S. Teramoto (Keio University School of Medicine) for technical assistance.

References

Abbott, D.H., Barnett, D.K., Colman, R.J., Yamamoto, M.E., Schultz-Darken, N.J., 2003. Aspects of common marmoset basic biology and life history important for biomedical research. Comp. Med. 53 (4), 339–350.

Babatz, J., Rollig, C., Oelschlagel, U., Zhao, S., Ehninger, G., Schmitz, M., Bornhauser, M., 2003. Large-scale immunomagnetic selection of CD14+ monocytes to generate dendritic cells for cancer immunotherapy: a phase I study. J. Hematother. Stem Cell Res. 12 (5), 515–523.

Banchereau, J., Palucka, A.K., 2005. Dendritic cells as therapeutic vaccines against cancer. Nat. Rev. Immunol. 5 (4), 296–306.

Barros, M., Boere, V., Huston, J.P., Tomaz, C., 2000. Measuring fear and anxiety in the marmoset (*Callithrix penicillata*) with a novel predator confrontation model: effects of diazepam. Behav. Brain Res. 108 (2), 205–211.

Batchelor, P.E., Liberatore, G.T., Wong, J.Y., Porritt, M.J., Frerichs, F., Donnan, G.A., Howells, D.W., 1999. Activated macrophages and microglia induce dopaminergic sprouting in the injured striatum and express brain-derived neurotrophic factor and glial cell line-derived neurotrophic factor. J. Neurosci. 19 (5), 1708–1716.

Bouhy, D., Malgrange, B., Multon, S., Poirrier, A.L., Scholtes, F., Schoenen, J., Franzen, R., 2006. Delayed GM-CSF treatment stimulates axonal regeneration and functional recovery in paraplegic rats via an increased BDNF expression by endogenous macrophages. FASEB J. 20 (8), 1239–1241.

Courtine, G., Bunge, M.B., Fawcett, J.W., Grossman, R.G., Kaas, J.H., Lemon, R., Maier, I., Martin, J., Nudo, R.J., Ramon-Cueto, A., Rouiller, E.M., Schnell, L., Wannier, T., Schwab, M.E., Edgerton, V.R., 2007. Can experiments in nonhuman primates expedite the translation of treatments for spinal cord injury in humans? Nat. Med. 13 (5), 561–566.

Cummings, B.J., Uchida, N., Tamaki, S.J., Salazar, D.L., Hooshmand, M., Summers, R., Gage, F.H., Anderson, A.J., 2005. Human neural stem cells differentiate and promote locomotor recovery in spinal cord-injured mice. Proc. Natl. Acad. Sci. U.S.A. 102 (39), 14069–14074.

Doucette, R., 1995. Olfactory ensheathing cells: potential for glial cell transplantation into areas of CNS injury. Histol. Histopathol. 10 (2), 503–507.

Elkabes, S., DiCicco-Bloom, E.M., Black, I.B., 1996. Brain microglia/macrophages express neurotrophins that selectively regulate microglial proliferation and function. J. Neurosci. 16 (8), 2508–2521.

Fouad, K., Klusman, I., Schwab, M.E., 2004. Regenerating corticospinal fibers in the Marmoset (*Callithrix jacchus*) after spinal cord lesion and treatment with the anti-Nogo-A antibody IN-1. Eur. J. Neurosci. 20 (9), 2479–2482.

Fujiyoshi, K., Yamada, M., Nakamura, M., Yamane, J., Katoh, H., Kitamura, K., Kawai, K., Okada, S., Momoshima, S., Toyama, Y., Okano, H., 2007. In vivo tracing of neural tracts in the intact and injured spinal cord of marmosets by diffusion tensor tractography. J. Neurosci. 27 (44), 11991–11998.

Girard, C., Bemelmans, A.P., Dufour, N., Mallet, J., Bachelin, C., Nait-Oumesmar, B., Baron-Van Evercooren, A., Lachapelle, F., 2005. Grafts of brain-derived neurotrophic factor and neurotrophin 3-transduced primate Schwann cells lead to functional recovery of the demyelinated mouse spinal cord. J. Neurosci. 25 (35), 7924–7933.

Gnanalingham, K.K., Smith, L.A., Hunter, A.J., Jenner, P., Marsden, C.D., 1993. Alterations in striatal and extrastriatal D-1 and D-2 dopamine receptors in the MPTP-treated common marmoset: an autoradiographic study. Synapse 14 (2), 184–194.

Grill, R., Murai, K., Blesch, A., Cage, F.H., Tuszynski, M.H., 1997. Cellular delivery of neurotrophin-3 promotes corticospinal axonal growth and partial functional recovery after spinal cord injury. J. Neurosci. 17 (4), 5560–5572.

Hauben, E., Nevo, U., Yoles, E., Moalem, G., Agranov, E., Mor, F., Akselrod, S., Neeman, M., Cohen, I.R., Schwartz, M., 2000. Autoimmune T cells as potential neuroprotective therapy for spinal cord injury. Lancet 355 (9200), 286–287.

Iarikov, D.E., Kim, B.G., Dai, H.N., McAtee, M., Kuhn, P.L., Bregman, B.S., 2007. Delayed transplantation with exogenous neurotrophin administration enhances plasticity of corticofugal projections after spinal cord injury. J. Neurotrauma 24 (4), 690–702.

Iwanami, A., Kaneko, S., Nakamura, M., Kanemura, Y., Mori, H., Kobayashi, S., Yamasaki, M., Momoshima, S., Ishii, H., Ando, K., Tanioka, Y., Tamaoki, N., Nomura, T., Toyama, Y., Okano, H., 2005a. Transplantation of human neural stem cells for spinal cord injury in primates. J. Neurosci. Res. 80 (2), 182–190.

Iwanami, A., Yamane, J., Katoh, H., Nakamura, M., Momoshima, S., Ishii, H., Tanioka, Y., Tamaoki, N., Nomura, T., Toyama, Y., Okano, H., 2005b. Establishment of graded spinal cord injury model in a nonhuman primate: the common marmoset. J. Neurosci. Res. 80 (2), 172–181.

Kendall, A.L., Rayment, F.D., Torres, E.M., Baker, H.F., Ridley, R.M., Dunnett, S.B., 1998. Functional integration of striatal allografts in a primate model of Huntington's disease. Nat. Med. 4 (6), 727–729.

Knoller, N., Auerbach, G., Fulga, V., Zelig, G., Attias, J., Bakimer, R., Marder, J.B., Yoles, E., Belkin, M., Schwartz, M., Hadani, M., 2005. Clinical experience using incubated autologous macrophages as a treatment for complete spinal cord injury: phase I study results. J. Neurosurg. Spine 3 (3), 173–181.

Koda, M., Okada, S., Nakayama, T., Koshizuka, S., Kamada, T., Nishio, Y., Someya, Y., Yoshinaga, K., Okawa, A., Moriya, H., Yamazaki, M., 2005. Hematopoietic stem cell and marrow stromal cell for spinal cord injury in mice. Neuroreport 16 (16), 1763–1767.

Koshizuka, S., Okada, S., Okawa, A., Koda, M., Murasawa, M., Hashimoto, M., Kamada, T., Yoshinaga, K., Murakami, M., Moriya, H., Yamazaki, M., 2004. Transplanted hematopoietic stem cells from bone marrow differentiate into neural lineage cells and promote functional recovery after spinal cord injury in mice. J. Neuropathol. Exp. Neurol. 63 (1), 64–72.

Lemon, R.N., Kirkwood, P.A., Maier, M.A., Nakajima, K., Nathan, P., 2004. Direct and indirect pathways for corticospinal control of upper limb motoneurons in the primate. Prog. Brain Res. 143, 263–279.

Liu, S., Aghakhani, N., Boisset, N., Said, G., Tadie, M., 2001. Innervation of the caudal denervated ventral roots and their target muscles by the rostral spinal motoneurons after implanting a nerve autograft in spinal cord-injured adult marmosets. J. Neurosurg. 94 (1 Suppl.), 82–90.

Ludlage, E., Mansfield, K., 2003. Clinical care and diseases of the common marmoset (*Callithrix jacchus*). Comp. Med. 53 (4), 369–382.

Mansfield, K., 2003. Marmoset models commonly used in biomedical research. Comp. Med. 53 (4), 383–392.

Marshall, J.W., Cross, A.J., Jackson, D.M., Green, A.R., Baker, H.F., Ridley, R.M., 2000. Clomethiazole protects against hemineglect in a primate model of stroke. Brain Res. Bull. 52 (1), 21–29.

Martin, D., Robe, P., Franzen, R., Delree, P., Schoenen, J., Stevenaert, A., Moonen, G., 1996. Effects of Schwann cell transplantation in a contusion model of rat spinal cord injury. J. Neurosci. Res. 45 (5), 588–597.

McDonald, J.W., Liu, X.Z., Qu, Y., Liu, S., Mickey, S.K., Turetsky, D., Gottlieb, D.I., Choi, D.W., 1999. Transplanted embryonic stem cells survive, differentiate and promote recovery in injured rat spinal cord. Nat. Med. 5 (12), 1410–1412.

McTigue, D.M., Horner, P.J., Stokes, B.T., Gage, F.H., 1998. Neurotrophin-3 and brain-derived neurotrophic factor induce oligodendrocyte proliferation and myelination of regenerating axons in the contused adult rat spinal cord. J. Neurosci. 18, 5354–5365.

Metz, G.A., Curt, A., van de Meent, H., Klusman, I., Schwab, M.E., Dietz, V., 2000. Validation of the weight-drop contusion model in rats: a comparative study of human spinal cord injury. J. Neurotrauma 17 (1), 1–17.

Mikami, Y., Okano, H., Sakaguchi, M., Nakamura, M., Shimazaki, T., Okano, H.J., Kawakami, Y., Toyama, Y., Toda, M., 2004. Implantation of dendritic cells in injured adult spinal cord results in activation of endogenous neural stem/progenitor cells leading to de novo neurogenesis and functional recovery. J. Neurosci. Res. 76 (4), 453–465.

Miwa, T., Furukawa, S., Nakajima, K., Furukawa, Y., Kohsaka, S., 1997. Lipopolysaccharide enhances synthesis of brain-derived neurotrophic factor in cultured rat microglia. J. Neurosci. Res. 50 (6), 1023–1029.

Motta, M.R., Castellani, S., Rizzi, S., Curti, A., Gubinelli, F., Fogli, M., Ferri, E., Cellini, C., Baccarani, M., Lemoli, R.M., 2003. Generation of dendritic cells from CD14+ monocytes positively selected by immunomagnetic adsorption for multiple myeloma patients enrolled in a clinical trial of anti-idiotype vaccination. Br. J. Haematol. 121 (2), 240–250.

Nakajima, K., Honda, S., Tohyama, Y., Imai, Y., Kohsaka, S., Kurihara, T., 2001. Neurotrophin secretion from cultured microglia. J. Neurosci. Res. 65 (4), 322–331.

Nencioni, A., Brossart, P., 2004. Cellular immunotherapy with dendritic cells in cancer: current status. Stem Cells 22 (4), 501–513.

Ogawa, Y., Sawamoto, K., Miyata, T., Miyao, S., Watanabe, M., Nakamura, M., Bregman, B.S., Koike, M., Uchiyama, Y., Toyama, Y., Okano, H., 2002. Transplantation of in vitro-expanded fetal neural progenitor cells results in neurogenesis and functional recovery after spinal cord contusion injury in adult rats. J. Neurosci. Res. 69 (6), 925–933.

Ohta, S., Ueda, Y., Yaguchi, M., Matsuzaki, Y., Nakamura, M., Toyama, Y., Tanioka, Y., Tamaoki, N., Nomura, T., Okano, H., Kawakami, Y., Toda, M., 2008. Isolation and characterization of dendritic cells from common marmosets for preclinical cell therapy studies. Immunology 123 (4), 566–574.

Okada, S., Ishii, K., Yamane, J., Iwanami, A., Ikegami, T., Katoh, H., Iwamoto, Y., Nakamura, M., Miyoshi, H., Okano, H.J., Contag, C.H., Toyama, Y., Okano, H., 2005. In vivo imaging of engrafted neural stem cells: its application in evaluating the optimal timing of transplantation for spinal cord injury. FASEB J. 19 (13), 1839–1841.

Okano, H., 2002. Stem cell biology of the central nervous system. J. Neurosci. Res. 69 (6), 698–707.

Prewitt, C.M., Niesman, I.R., Kane, C.J., Houle, J.D., 1997. Activated macrophage/microglial cells can promote the regeneration of sensory axons into the injured spinal cord. Exp. Neurol. 148 (2), 433–443.

Rabchevsky, A.G., Streit, W.J., 1997. Grafting of cultured microglial cells into the lesioned spinal cord of adult rats enhances neurite outgrowth. J. Neurosci. Res. 47 (1), 34–48.

Richter, M.W., Roskams, A.J., 2008. Olfactory ensheathing cell transplantation following spinal cord injury: hype or hope? Exp. Neurol. 209 (2), 353–367.

Schuler, G., Schuler-Thurner, B., Steinman, R.M., 2003. The use of dendritic cells in cancer immunotherapy. Curr. Opin. Immunol. 15 (2), 138–147.

Steinman, R.M., 1991. The dendritic cell system and its role in immunogenicity. Annu. Rev. Immunol. 9, 271–296.
Steinman, R.M., Hawiger, D., Nussenzweig, M.C., 2003. Tolerogenic dendritic cells. Annu. Rev. Immunol. 21, 685–711.
t Hart, B.A., Bauer, J., Muller, H.J., Melchers, B., Nicolay, K., Brok, H., Bontrop, R.E., Lassmann, H., Massacesi, L., 1998. Histopathological characterization of magnetic resonance imaging-detectable brain white matter lesions in a primate model of multiple sclerosis: a correlative study in the experimental autoimmune encephalomyelitis model in common marmosets (*Callithrix jacchus*). Am. J. Pathol. 153 (2), 649–663.
t Hart, B.A., Laman, J.D., Bauer, J., Blezer, E., van Kooyk, Y., Hintzen, R.Q., 2004. Modelling of multiple sclerosis: lessons learned in a non-human primate. Lancet Neurol. 3 (10), 588–597.
Takami, T., Oudega, M., Bates, M.L., Wood, P.M., Kleitman, N., Bunge, M.B., 2002. Schwann cell but not olfactory ensheathing glia transplants improve hindlimb locomotor performance in the moderately contused adult rat thoracic spinal cord. J. Neurosci. 22 (15), 6670–6681.
Terashima, T., Ochiishi, T., Yamauchi, T., 1994. Immunohistochemical detection of calcium/calmodulin-dependent protein kinase II in the spinal cord of the rat and monkey with special reference to the corticospinal tract. J. Comp. Neurol. 340 (4), 469–479.
Yoon, S.H., Shim, Y.S., Park, Y.H., Chung, J.K., Nam, J.H., Kim, M.O., Park, H.C., Park, S.R., Min, B.H., Kim, E.Y., Choi, B.H., Park, H., Ha, Y., 2007. Complete spinal cord injury treatment using autologous bone marrow cell transplantation and bone marrow stimulation with granulocyte macrophage-colony stimulating factor (GM-CSF): phase i/ii clinical trial. Stem Cells 25 (8), 2066–2073.

Roles of ES Cell-Derived Gliogenic Neural Stem/Progenitor Cells in Functional Recovery after Spinal Cord Injury

Gentaro Kumagai[1,2,3], Yohei Okada[1,4,5], Junichi Yamane[2], Narihito Nagoshi[1,2], Kazuya Kitamura[1,2], Masahiko Mukaino[1,6], Osahiko Tsuji[1,2], Kanehiro Fujiyoshi[1,2], Hiroyuki Katoh[2], Seiji Okada[7], Shinsuke Shibata[1], Yumi Matsuzaki[1], Satoshi Toh[3], Yoshiaki Toyama[2], Masaya Nakamura[2]*, Hideyuki Okano[1]*

1 Department of Physiology, Keio University School of Medicine, Tokyo, Japan, 2 Department of Orthopedic Surgery, Keio University School of Medicine, Tokyo, Japan, 3 Department of Orthopedic Surgery, Hirosaki University Graduate School of Medicine, Hirosaki, Japan, 4 Department of Neurology, Graduate School of Medicine, Nagoya University, Nagoya, Japan, 5 Kanrinmaru Project, Keio University School of Medicine, Tokyo, Japan, 6 Department of Rehabilitation Medicine, Keio University School of Medicine, Tokyo, Japan, 7 Department of Research Super Star Program Stem Cell Unit, Graduate School of Medical Science, Kyusyu University, Fukuoka, Japan

Abstract

Transplantation of neural stem/progenitor cells (NS/PCs) following the sub-acute phase of spinal cord injury (SCI) has been shown to promote functional recovery in rodent models. However, the types of cells most effective for treating SCI have not been clarified. Taking advantage of our recently established neurosphere-based culture system of ES cell-derived NS/PCs, in which primary neurospheres (PNS) and passaged secondary neurospheres (SNS) exhibit neurogenic and gliogenic potentials, respectively, here we examined the distinct effects of transplanting neurogenic and gliogenic NS/PCs on the functional recovery of a mouse model of SCI. ES cell-derived PNS and SNS transplanted 9 days after contusive injury at the Th10 level exhibited neurogenic and gliogenic differentiation tendencies, respectively, similar to those seen *in vitro*. Interestingly, transplantation of the gliogenic SNS, but not the neurogenic PNS, promoted axonal growth, remyelination, and angiogenesis, and resulted in significant locomotor functional recovery after SCI. These findings suggest that gliogenic NS/PCs are effective for promoting the recovery from SCI, and provide essential insight into the mechanisms through which cellular transplantation leads to functional improvement after SCI.

Citation: Kumagai G, Okada Y, Yamane J, Nagoshi N, Kitamura K, et al. (2009) Roles of ES Cell-Derived Gliogenic Neural Stem/Progenitor Cells in Functional Recovery after Spinal Cord Injury. PLoS ONE 4(11): e7706. doi:10.1371/journal.pone.0007706

Editor: Kenji Hashimoto, Chiba University Center for Forensic Mental Health, Japan

Received August 18, 2009; **Accepted** October 9, 2009; **Published** November 6, 2009

Funding: This work was supported by grants from the Leading Project for Realization of Regenerative Medicine from the Ministry of Education, Culture, Sports, Science and Technology (MEXT) of Japan; Japan Science and Technology Agency (SORST); the Ministry of Health, Labor, and Welfare (to H. O.); the General Insurance Association of Japan (to M.N. and Y.T; this is not a commercial entity); Research Fellowships for Young Scientists from the Japan Society for the Promotion of Science (to Y. O.); Keio Gijuku Academic Development Funds; and by a Grant-in-aid for Global COE Program from MEXT to Keio University. The funders had no role in study design, data collection and analysis, decision to publish, or preparation of the manuscript.

Competing Interests: The authors have declared that no competing interests exist.

* E-mail: hidokano@sc.itc.keio.ac.jp (HO); masa@sc.itc.keio.ac.jp (MN)

Introduction

Because the adult central nervous system (CNS) has limited potential for regeneration, spinal cord injury (SCI) results in severe dysfunction, such as paraplegia and tetraplegia. With the aim of regenerating the injured spinal cord, various intraspinal cellular transplants have been investigated, especially in the sub-acute phase after injury. This period, between the acute and chronic phases, is marked by the minimal expression of cytokines, and is likely to be amenable to transplantation therapy [1,2,3,4,5]. Embryonic stem (ES) cells, with their indefinite replication potential, pluripotency, and genetic flexibility, have attracted great interest, and methods for inducing their neural differentiation have been extensively studied [6]. ES cell-derived neural progenitors are currently one of the most promising cell sources for cell transplantation therapy for treating SCI. Although previous studies demonstrated that the transplantation of mouse ES cell-derived embryoid bodies [7] or human ES cell-derived oligodendrocyte progenitor cells [8] promotes overall functional recovery after SCI, the types of neural progenitor cells most effective for treating sub-acute phase SCI has been uncertain.

We recently reported that a low concentration of retinoic acid (10^{-8} M: low-RA) can efficiently induce caudalized neural progenitors in embryoid bodies (EBs) [9], and we established a neurosphere-based culture system of ES cell-derived neural stem/progenitor cells (NS/PCs) from low-RA-treated EBs, with midbrain to hindbrain identities [10]. These ES cell-derived primary neurospheres (PNS) mainly exhibit neurogenic differentiation potentials, whereas passaged secondary neurospheres (SNS) are more gliogenic, corresponding to changes in CNS development, in which neurogenic NS/PCs predominate early in gestation and gliogenic NS/PCs predominate in mid-to-late gestation. Here, taking advantage of this difference between neurogenic PNS and gliogenic SNS, we transplanted PNS and SNS into the injured spinal cord, examined the differentiation and growth properties of the grafted cells, and compared their effects on angiogenesis, axonal regeneration, and functional recovery after SCI. We also examined the survival and growth of the

transplanted ES cell-derived NS/PCs using *in vivo*, live, bioluminescent imaging (BLI) to evaluate the tumorigenicity and safety of the grafted cells.

Results

Establishment of a Stable ES Cell Line Expressing CBR*luc* Luminescence and Venus Fluorescence

We first established an ES cell line that constitutively expresses the click beetle red-emitting luciferase (CBR*luc*) [11] and Venus [12] by introducing a CAG-CBR*luc*-IRES-Venus plasmid (Fig. 1**A**) into EB3 ES cells (CCV-ES cells) [13]. CCV-ES cells and their progenies were detected by both BLI [3,14,15] and fluorescence microscopy. To induce NS/PCs from ES cells and obtain PNS and SNS, we used a neurosphere-based culture system that we recently reported [10] (Fig. 1**B**), as described in Materials and Methods. More than 99% of the undifferentiated CCV-ES cells expressed Venus fluorescence by flow cytometry (Fig. 1**D and E**), and CCV-ES cell-derived PNS (CCV-PNS) and SNS (CCV-SNS) showed steady fluorescence that was detectable by fluorescence microscopy (Fig. 1**C**). Approximately 80% of the cells in the CCV-PNS and -SNS were positive for Venus by flow cytometry (Fig. 1**D and E**). bioluminescence imaging (BLI) revealed CBR*luc* expression in both CCV-PNS and –SNS, and we confirmed that the photon counts were in direct proportion to the cell numbers *in vitro* (Fig. 1**F**). We also confirmed that the CCV-ES cells could generate PNS and SNS similar to EB3-ES cells (Fig. 1**C**).

Distinct Differentiation Potentials of PNS and SNS *In Vitro*

We next examined the *in vitro* differentiation potentials of the PNS and SNS derived from EB3- and CCV-ES cells. PNS and SNS derived from EB3- and CCV-ES cells were allowed to differentiate in medium without FGF2 on poly-L-ornithine/fibronectin coated coverslips for 5 days, and then processed for immunocytochemistry. We examined the frequency of colonies consisting of βIII tubulin-positive neurons, GFAP-positive astrocytes, and/or O4-positive oligodendrocytes, and found that the EB3- and CCV-PNS colonies predominantly differentiated into neurons, although a small number of colonies contained both neurons and glia (Fig. 1**G**). In contrast, most of the EB3- and CCV-SNS colonies differentiated into both neurons and glia, including astrocytes and oligodendrocytes, or into only glial cells (Fig. 1**G**), demonstrating that the ES cell-derived PNS and SNS had distinct differentiation potentials *in vitro* (Fig. 1**H**). Moreover, EB3- and CCV-ES cell-derived neurospheres exhibited similar differentiation properties, confirming that the transgene in the ES cells had negligible effects on differentiation (Fig. 1**H**).

We also examined the SNS formation rates to determine the self-renewing ability of the ES cell-derived PNS. We cultured CCV-PNS at a low cell density (2.5×10^4 cells/ml), transferred them into 96-well plates at one neurosphere/well, dissociated the neurospheres, and cultured them again with FGF2 to form secondary neurospheres. Most of the CCV-PNS generated secondary neurospheres (79/90; 87.7%; from more than three independent experiments), confirming their ability to self-renew.

Transplanted SNS Prevented Atrophic Change and Demyelination after SCI

A contusive SCI was induced at the Th10 level of C57BL6 mice, and 5×10^5 cells of CCV-PNS or CCV-SNS, or PBS as a control, were injected into the lesion epicenter 9 days after injury. We refer to these, respectively, as the PNS, SNS, and control groups. After 6 weeks, histological analyses were performed. We first examined atrophic changes of the injured spinal cord by Hematoxylin-eosin (H–E) staining (Fig. 2**A and B**). The transverse area of the spinal cord at the lesion epicenter was significantly larger in the SNS group than in the control group, suggesting that SNS transplantation prevented atrophy of the injured spinal cord (Fig. 2**E**). Luxol Fast Blue (LFB) staining revealed significantly greater preservation of the myelinated areas in the SNS group compared with the control (both 2 and 6 weeks after injury) and PNS groups (Fig. 2**C and D**), from 1 mm rostral to 1 mm caudal to the epicenter (Fig. 2F). Notably, there was a significantly spared rim of white matter in the SNS group, even at the lesion epicenter, whereas the control group exhibited severely demyelinated white matter throughout the lesioned area (2 mm rostral and caudal to the lesion epicenter) (Fig. 2**C and D**).

Transplanted PNS and SNS survived in the injured spinal cord and did not form tumors

The photon count measured by bioluminescence imaging (BLI) quantifies only living cells, since the luciferin-CBR-luciferase reaction depends on oxygen and ATP. The successful transplantation of CCV-PNS and -SNS was confirmed immediately after transplantation using BLI, and the average signal intensity was $2.2\pm1.6\times10^5$ photons/mouse/sec in 22 transplanted mice. Images obtained weekly thereafter for 6 weeks showed that the signal intensity dropped sharply within the first week after transplantation, but remained at 20% of the initial photon count in both the PNS and SNS transplantation groups throughout the remaining period. Although the signal intensity at 1 week was significantly higher in the PNS group (62.4%) than in the SNS group (29.5%), there was no significant difference in the signal intensity between the PNS (12.6%) and SNS (18.9%) groups at 6 weeks, suggesting there was a similar number of live grafted PNS- and SNS-derived cells within the injured spinal cord 6 weeks after transplantation. Thus, similar numbers of grafted PNS and SNS cells may have survived in the injured spinal cord, although the possibility that the grafted cells proliferated differently in the two groups 1 to 6 weeks after transplantation cannot be excluded. Notably, a rapid increase in signal intensity, which would have suggested tumor formation, was not observed during this time period (Fig. 3**A and B**). Consistently, histological analysis confirmed that both the CCV-PNS- and CCV-SNS-derived Venus-positive cells survived without forming tumors (Fig. 3**C–F**). Quantitative analysis of the Venus-positive area revealed that there was no significant difference of the number of survived grafted cells between PNS and SNS groups 6 weeks after transplantation (Fig. 3**G**). Moreover, the data of BLI correlated well with Venus-positive area (Pearson's correlation coefficient: 0.759, $p=0.04$, Fig. 3**H**).

PNS and SNS Grafted onto Injured Spinal Cord Exhibited Differentiation Potentials Similar to Those Observed *In Vitro*

To examine the differentiation characteristics of CCV-PNS and -SNS grafted onto the injured spinal cord, we performed immunohistochemical analyses, and determined the proportion of cells immunopositive for each cell type-specific marker among the Venus-positive grafted cells [3]. Both the PNS- and SNS-derived cells integrated at or near the lesion epicenter and differentiated into Hu-positive neurons, GFAP-positive astrocytes, and APC-positive oligodendrocytes (Fig. 4**A–E**). The percentage of Hu/Venus double-positive neurons in the PNS group ($52.8\pm19.1\%$) was three times that in the SNS group ($16.3\pm5.2\%$) (Fig. 4**F**). In contrast, the percentage of GFAP/Venus double-positive astrocytes or APC/Venus double-positive

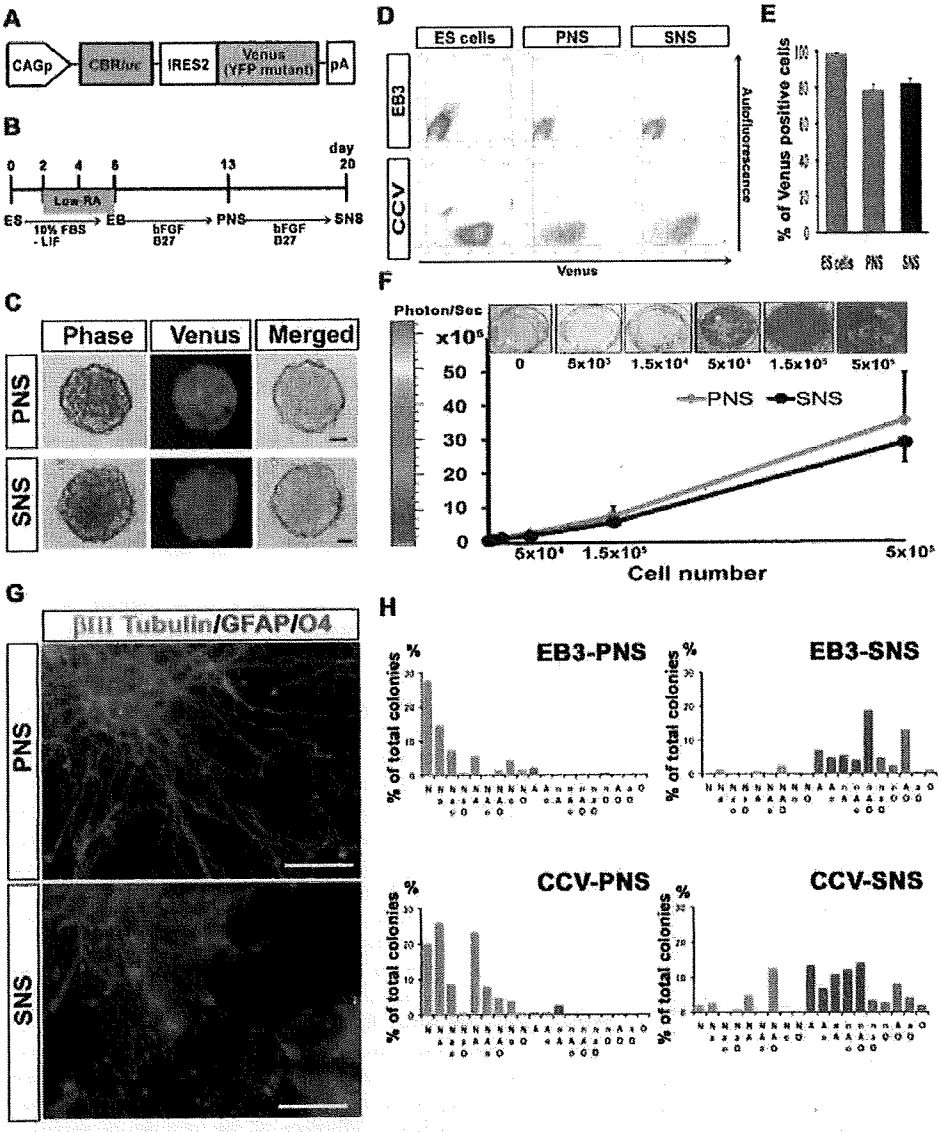

Figure 1. Establishment of a stable ES cell line expressing CBR/*luc* luminescence and Venus fluorescence, and their differentiation analysis. (A) The CAG-CBR/*luc*-IRES-Venus gene (CCV) construct. (B) Protocols for deriving neurospheres from mouse ES cells. ES cells were dissociated into single cells with 0.25% trypsin-EDTA and cultured for 6 days to allow the formation of embryoid bodies (EBs). A low concentration of RA was added on day 2 of EB formation for neural induction. The EBs were dissociated into single cells with 0.25% trypsin-EDTA and cultured in suspension for 7 days, to obtain primary neurospheres (ES cell-derived primary neurospheres, PNS). These PNS were dissociated into single cells with TripleLE Select (Invitrogen) and cultured again in suspension for 7 days under the same conditions to form secondary neurospheres (SNS). (C) Images of CCV-PNS and -SNS visualized by fluorescence microscopy. Scale bar: 100 μm. (D) Flow cytometric analysis of Venus-positive cells in PNS and SNS derived from CCV- and EB3-ES cells. (E) The proportion of Venus-positive cells among CCV-ES cells and their progenies, CCV-PNS and -SNS. Approximately 80% of the CCV-PNS and -SNS cells were positive for Venus. Values are means ± s.e.m. ($n=3$). (F) Correlation between the cell numbers of CCV-PNS and -SNS, and the measured photon counts. BLI revealed CBR*luc* expression in both CCV-PNS and -SNS, and we determined that the photon counts were in direct proportion to the cell numbers *in vitro*. Values are means ± s.e.m. ($n=3$). (G)(H) Distinct differentiation potentials of PNS and SNS *in vitro*. Immunocytochemical analysis of βIII tubulin-positive neurons (N or n), GFAP-positive astrocytes (A or a), and O4-positive oligodendrocytes (O or o) (N, A, O: more than 20 cells; n, a, o: fewer than 19 cells in each colony, respectively). A neuron-only colony (N) and a colony consisting of astrocytes and oligodendrocytes (AO) are shown (G). Scale bar: 50 μm. Quantitative analysis of the *in vitro* differentiation potential of EB3-PNS and -SNS and CCV-PNS and -SNS, shown as the percentage of each phenotypic colony among the total colonies (H). The PNS colonies dominantly differentiated into neurons, while a small number of colonies contained glial cells. On the other hand, most of the SNS colonies differentiated into both neurons and glial cells, including astrocytes and oligodendrocytes, or into only glial cells. Values are means ± s.e.m. ($n=3$).
doi:10.1371/journal.pone.0007706.g001

oligodendrocytes in the SNS group (42.2±14.4, 33.6±5.4%) was twice that in the PNS group (19.0±9.3, 14.8±7.1%) (Fig. 4F) (n = 4). The differentiation patterns of the grafted PNS and SNS were consistent with the results of the *in vitro* differentiation assay, suggesting that PNS and SNS preserved their differentiation tendencies *in vivo*.

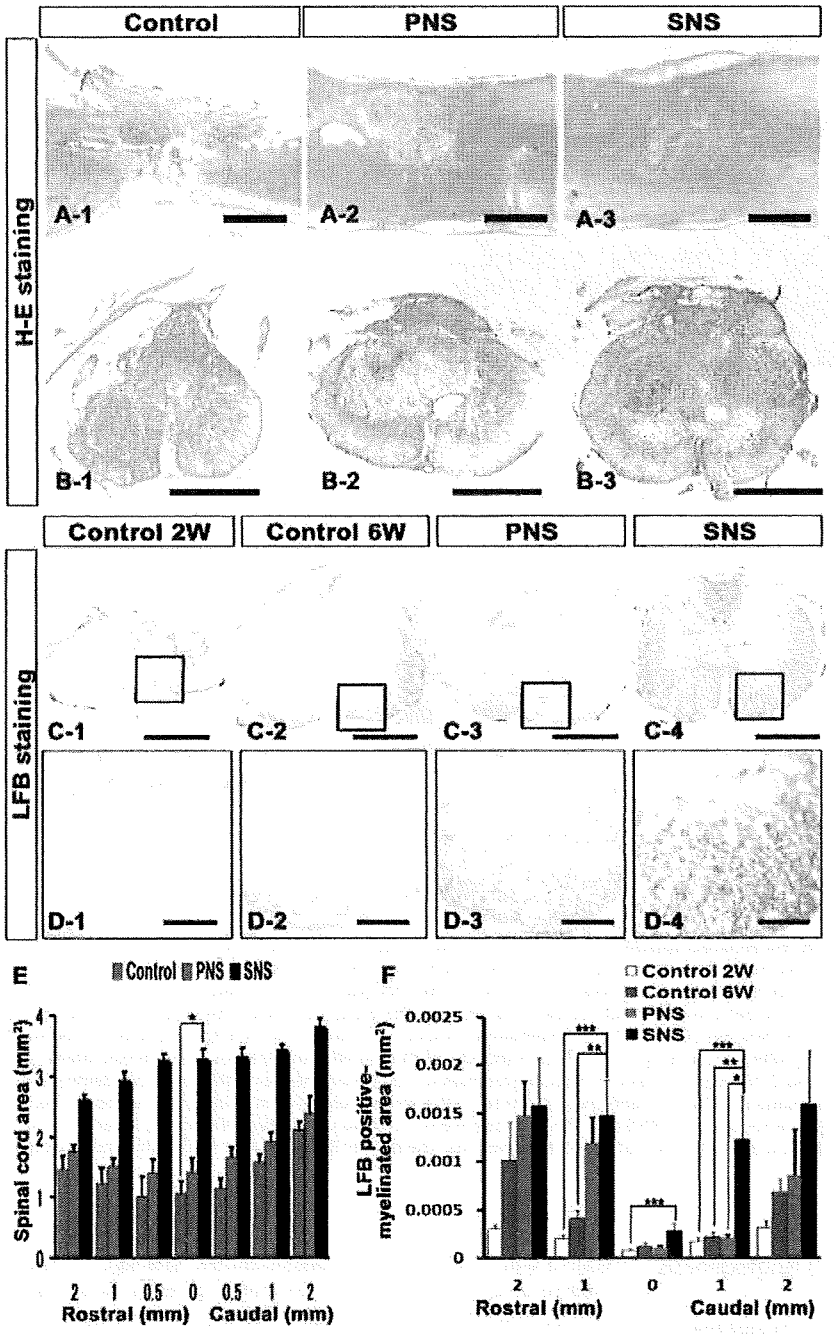

Figure 2. Transplanted SNS prevented atrophic change and demyelination after SCI. (A)(B) Representative H–E staining images of the sagittally sectioned (A1–3) and axially sectioned (B1–3) spinal cord at the lesion epicenter 6 weeks after injury. Scale bar: 500 μm. (C) Representative LFB staining images of the axially sectioned spinal cord 1 mm caudal to the lesion from each animal (2 weeks or 6 weeks after SCI for the vehicle-control group and 6 weeks after SCI for the PNS and SNS groups). Scale bar: 500 μm. (D) Higher magnification images of the boxed areas in C. Scale bar: 100 μm. (E) Quantitative analysis of the spinal cord area measured in H–E-stained axial sections through different regions. The transverse area of the spinal cord at the lesion epicenter was significantly larger in the SNS group compared with the control group. Values are means ± s.e.m. ($n = 5$). *: $P<0.05$, Control vs. SNS. (F) Quantitative analysis of the myelinated area by LFB-stained axial sections at different regions. LFB staining revealed greater preservation of myelination in the SNS group, with significant differences observed at the sites 1 mm rostral and 1 mm caudal to the epicenter compared with the control 2 or 6 weeks groups, 1 mm caudal to the epicenter compared with the PNS group, and at the epicenter compared with the control 2-week group. Values are means ± s.e.m. ($n = 5$). *: $P<0.05$, PNS vs. SNS. **: $P<0.05$, Control 6 weeks vs. SNS. ***: $P<0.05$, Control 2 weeks vs. SNS.

doi:10.1371/journal.pone.0007706.g002

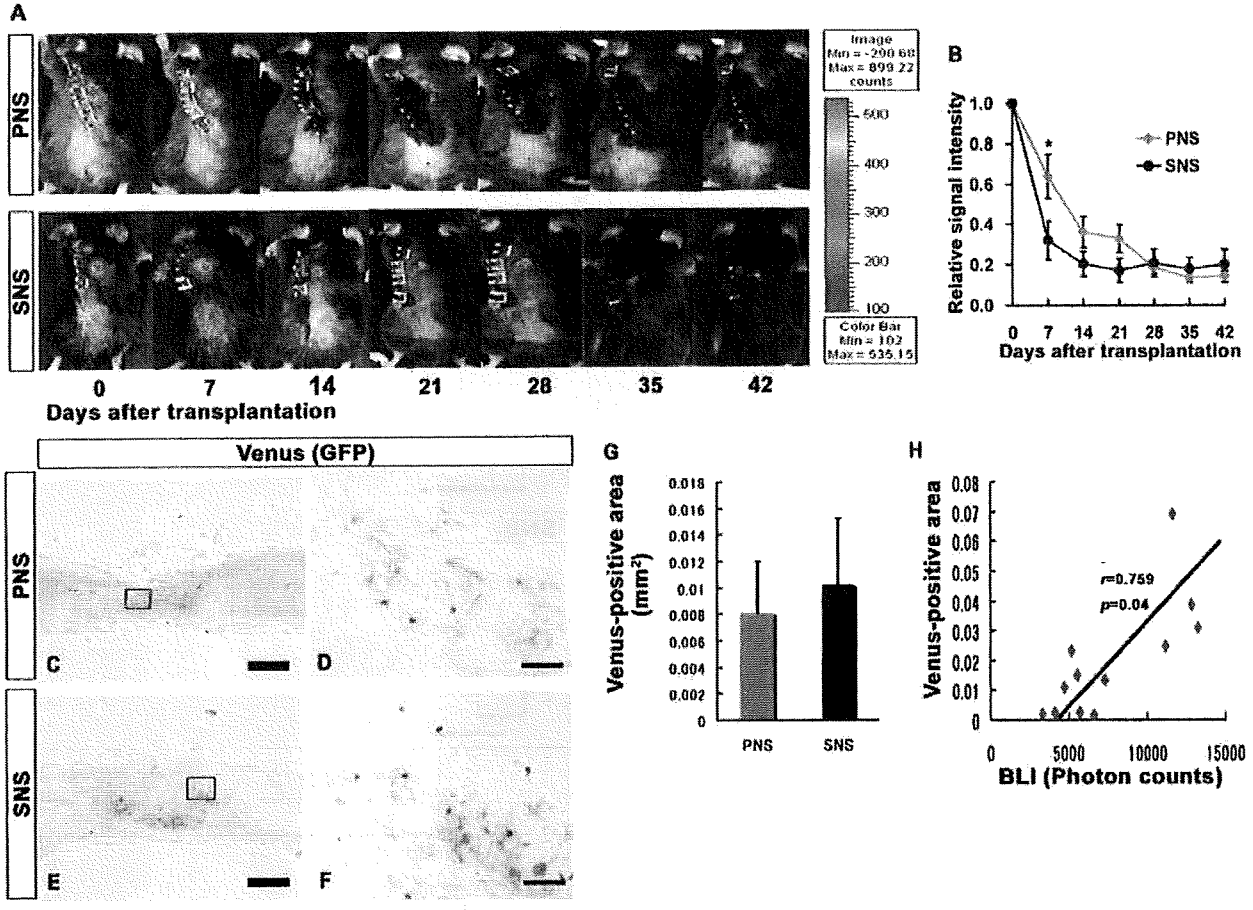

Figure 3. Transplanted PNS and SNS survived in the injured spinal cord and did not form tumors. (A) Representative BLI images of mice that received transplants of CCV-PNS and -SNS. (B) Signal intensity over time after transplantation in the PNS and SNS groups, shown relative to the initial value. Although the signal intensity at 1 week after the injury was significantly higher in the PNS group (62.4%) than the SNS group (29.5%), there was no significant difference in the signal intensity between the PNS (12.6%) and SNS (18.9%) groups 6 weeks after the injury. Values are means ± s.e.m. ($n = 11$). *: $P<0.05$, PNS vs. SNS. Scale bar: 500 μm. (C)(D)(E)(F) Representative images of sagittal sections of spinal cords grafted with PNS and SNS, which were immunostained for Venus (grafted cells) using an anti-GFP antibody. High-magnification images of the boxed areas in C and E are shown in D and F. Scale bar: 500 μm for C and E, 100 μm for D and F. Histological analysis confirmed that both PNS- and SNS-derived cells survived without forming tumors. (G) Quantitative analysis of Venus (GFP)-positive area at the lesion epicenter in midsagittal sections. Venus immunostaining revealed there was no significant difference between PNS and SNS groups 6 weeks after transplantation Values are means ± s.e.m. (n = 6). (H) Correlation of the results of BLI analysis and the quantification of Venus-positive area. The data of BLI correlated well with Venus-positive area (n = 12).
doi:10.1371/journal.pone.0007706.g003

Transplanted SNS, but Not PNS, Enhanced Angiogenesis after SCI

To examine the effects of CCV-PNS and -SNS transplantation on angiogenesis after SCI, sagittal and axial sections of the injured spinal cord were examined immunohistochemically for αSMA (a marker for smooth muscle cells) or PECAM-1 (a marker for endothelial cells). While a few αSMA-positive cells were observed at and near the lesion site in sagittal sections of both the control and PNS groups, significantly more αSMA-positive cells were found in the SNS group (Fig. 5**A and B**). These αSMA-positive cells accumulated near Venus-positive grafted cells (Fig. 5**C and D**). Similarly, significantly more PECAM-1-positive blood vessels were observed at the lesion site in the SNS group than in the PNS and control groups (Fig. 5**E–J, Y**). To clarify the underlying angiogenic signals, we examined the expression of an angiogenic growth factor, vascular endothelial growth factor (VEGF), in the grafted spinal cord by immunohistochemistry. Although a VEGF-positive area was observed at the lesion epicenter in all three groups 6 weeks after injury (Fig. 5**K–M**), it was significantly broader in the SNS group than in the other groups (Fig. 5**Z**). Furthermore, we found many GFAP/VEGF double-positive host astrocytes, which were negative for Venus (GFP) (Fig. 5**N–Q**), and a few Venus (GFP)/GFAP-positive graft-derived astrocytes expressing VEGF (Fig. 5**R–X**).

Transplanted SNS, but Not PNS, Promoted Axonal Regrowth and Enhanced Functional Recovery

To examine the effects of CCV-PNS and -SNS transplantation on axonal regrowth after SCI, we performed immunohistochemical analyses of the injured spinal cord for NF-H (RT97), 5-hydroxytryptamine (5-HT), and growth-associated protein-43 (GAP43). While few NF-H-positive axons were observed at the

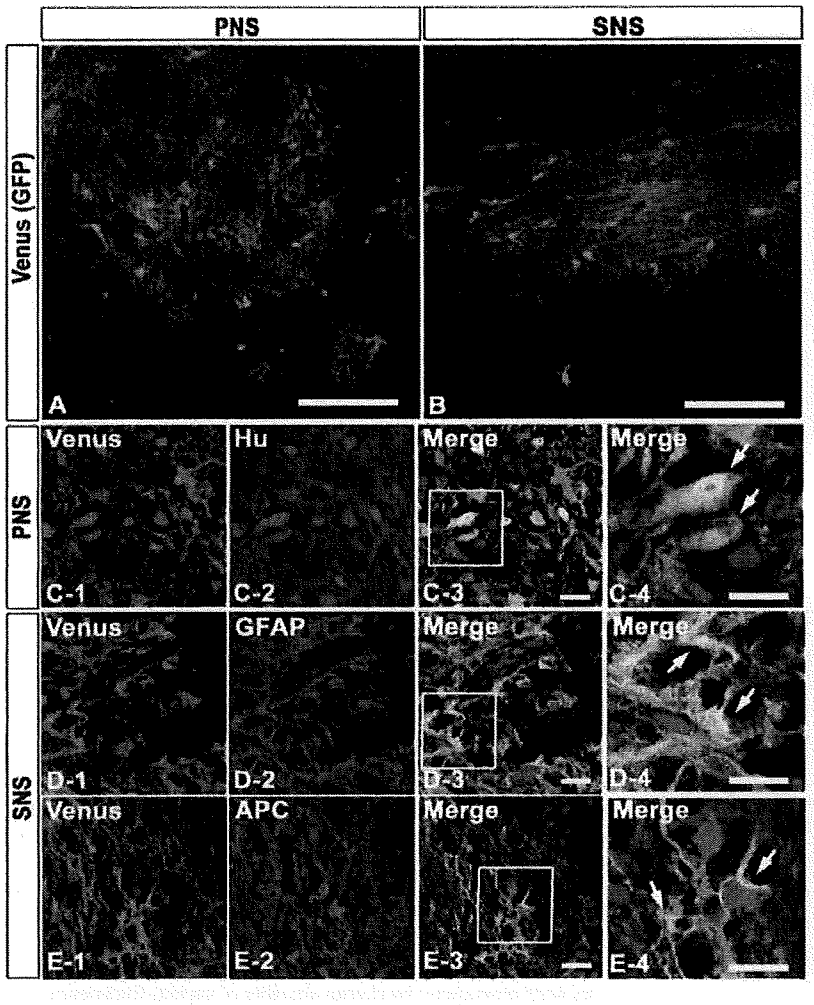

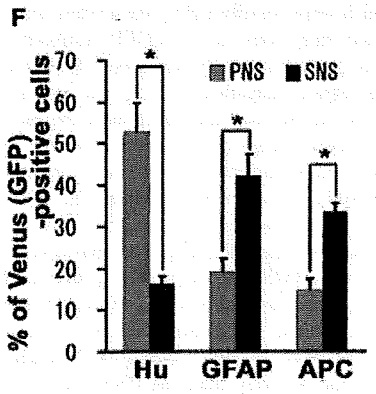

Figure 4. *In vivo* differentiation characteristics of PNS and SNS grafted onto the injured spinal cord. (A)(B) Venus-positive PNS- and SNS-derived grafted cells integrated at or near the lesion epicenter. Venus expression was detected by immunohistochemistry using an antibody against GFP. Scale bar 100 μm. (C)(D)(E) Representative immunohistochemical images of Venus-positive grafted cells that were positive for markers of neural lineages: Hu-positive neurons from PNS group (C), GFAP-positive astrocytes from SNS group (D), and APC-positive oligodendrocytes from SNS group (E). Scale bar: 20 μm. (C-4, D-4, E-4) Higher-magnification image of the boxed areas in C-3, D-3, E-3. Scale bar: 20 μm. (F) The percentage of cell type-specific marker positive cells among the Venus-positive grafted cells, showing the *in vivo* differentiation characteristics of PNS and SNS. The percentage of Hu-positive neurons in the PNS group (52.8±19.1%) was three times that in the SNS group (16.3±5.2%). In contrast, the percentage of GFAP-positive astrocytes or APC-positive oligodendrocytes in the SNS group (42.2±14.4, 33.6±5.4%) was twice that in the PNS group (19.0±9.3, 14.8±7.1%). Values are means ± s.e.m. ($n=4$). *: $P<0.05$, PNS vs. SNS.
doi:10.1371/journal.pone.0007706.g004

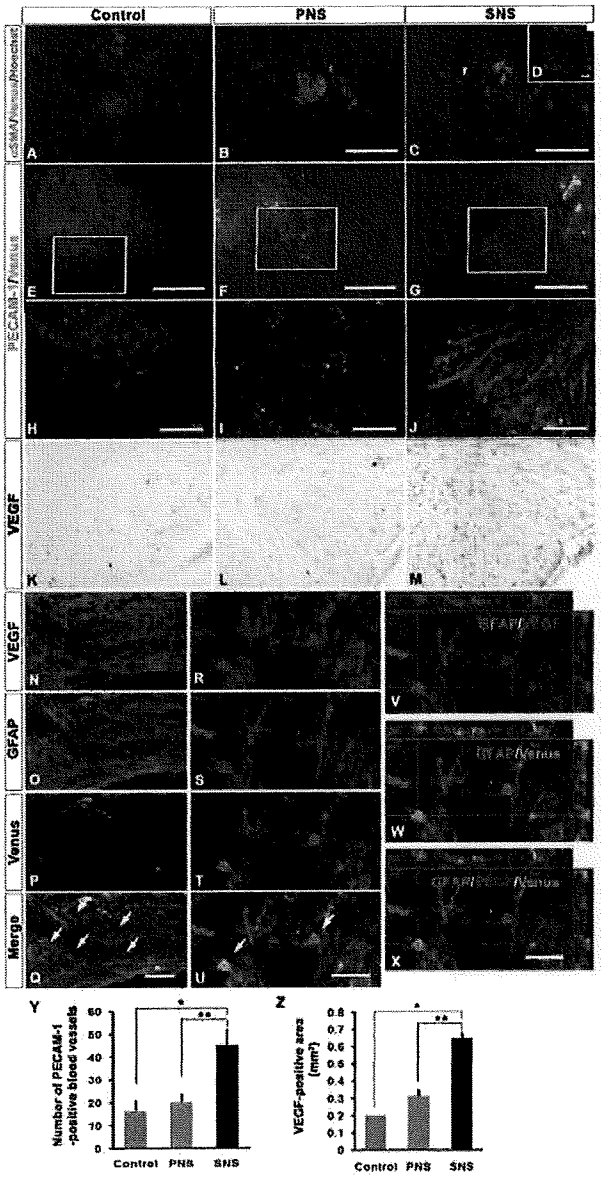

Figure 5. Transplanted SNS, but not PNS, enhanced angiogenesis after SCI. (A)(B)(C) Representative images of αSMA-immunostained sections obtained from the control (A), PNS (B), and SNS (C) groups. Scale bar: 500 μm. (D) Higher-magnification image of the area indicated by the arrowhead in C. Scale bar: 20 μm. While a few αSMA-positive Venus-expressing grafted cells were observed at and near the lesion site in sagittal sections of both the control and PNS groups, significantly more αSMA-positive cells were found in the SNS group, with Venus-positive grafted cells accumulated near the αSMA-positive cells, not colocalized with them. (E)(F)(G) Representative images of PECAM-1-immunostained sections obtained from the Control (E), PNS (F), and SNS (G) groups. Scale bar: 200 μm. (H)(I)(J) Higher-magnification images of the boxed areas in E, F, and G. Scale bar: 100 μm. (K)(L)(M) Representative images of axial sections stained for vascular endothelial growth factor (VEGF). Scale bar: 100 μm. (N–X) Expression of VEGF in GFAP-positive astrocytes among host-derived cells (N–Q) and Venus-positive (GFP immunostained) graft-derived cells (R–X) in the spinal cord from the SNS group (arrows indicate VEGF/GFAP double-positive cells). SNS transplants promoted VEGF expression in both the host- and graft-derived GFAP-positive astrocytes. Scale bar: 20 μm. (Y) Quantitative analysis of blood vessels at the lesion epicenter. PECAM-1 immunostaining revealed similar results, with significantly more PECAM-1-positive blood vessels observed at the lesion site in the SNS group compared with the PNS and control groups. Values are means ± s.e.m. (n = 3).*: $P<0.05$, Control vs. SNS. **: $P<0.05$, PNS vs. SNS. (Z) Quantitative analysis of the VEGF-positive area at the lesion epicenter. The VEGF-positive area at the lesion epicenter was significantly broader in the SNS group than in the other groups. Values are means ± s.e.m. (n = 3).*: $P<0.05$, Control vs. SNS. **: $P<0.05$, PNS vs. SNS.

doi:10.1371/journal.pone.0007706.g005

rim of the lesion epicenter in the control and PNS groups, there were significantly more NF-H-positive neuronal fibers in the SNS group at the lesion epicenter and perilesional area (Fig. 6**A, B, and E**). 5-HT-positive serotonergic fibers, which are descending raphespinal tract axons [16,17], were observed at the sites caudal to the lesion epicenter in all three groups 6 weeks after injury (Fig. 6**C**). Quantitative analysis revealed that there were significantly more 5-HT-positive fibers at the site 4 mm caudal to the lesion epicenter (Th10 level), which was approximately at the L1 level, in the SNS group compared with the other groups (Fig. 6F).

While few GAP43-positive axons [18,19,20] were detected caudal to the lesion epicenter in the control and PNS groups, there were significantly more GAP43-positive fibers in the SNS group in the ventral region 1 mm caudal to the lesion epicenter (Fig. 6**D, G**), suggesting that transplantation of the gliogenic SNS, but not of the neurogenic PNS, promoted axonal regeneration in the injured spinal cord.

We also observed NF-H-positive neuronal fibers extending along with the GFAP-positive immature astrocytes, which may have been partially derived from the grafted Venus-positive cells, and crossing the perilesional area in the SNS group (Fig. 7**A and B**). Furthermore, the SNS-derived Venus-positive cells differentiated into MBP-positive oligodendrocytes, which myelinated NF-H-positive fibers (Fig. 7**C**). Electron microscopy also revealed active remyelination in the SNS group (Fig. 7**D–F**). The grafted cells were in small groups containing 50–100 cells (Fig. 7**D**). The axons at these sites were enwrapped by myelin sheathes of various thicknesses and numbers of lamellae, which were contributed by the grafted cells, as confirmed by immunolabeling with an anti-GFP antibody to distinguish the transplanted cells from the locally surviving recipient cells (Fig. 7**E**). A much higher magnification revealed nanogold-labeled Venus-positive spots in the outer and inner mesaxons of the myelin cytoplasm. Some axons close to the lesion epicenter had undergone considerable re-myelination, and were enwrapped in spirals of more than ten layers of compacted lamellae (Fig. 7**F**).

Finally, we monitored the locomotor functional recovery in all three groups using the BMS scoring scale [21]. The contusive SCI resulted in complete paralysis (BMS score 0) on day 1, followed by gradual recovery with a plateau around 3 weeks. Although there was no significant difference in the BMS scores among the control, PNS, and SNS groups on day 14, the SNS group exhibited significantly better functional recovery than the PNS and control groups on day 21 and thereafter. On the other hand, there was no significant difference in the BMS scores between the PNS and control groups (Fig. 7**G**). From a clinical perspective, the recovery of the SNS group to levels exhibiting frequent to consistent weight-supported plantar steps and occasional forelimb-hindlimb coordination was especially noteworthy.

Discussion

Methods for effectively inducing neural differentiation from pluripotent ES cells have been extensively studied [6] and are

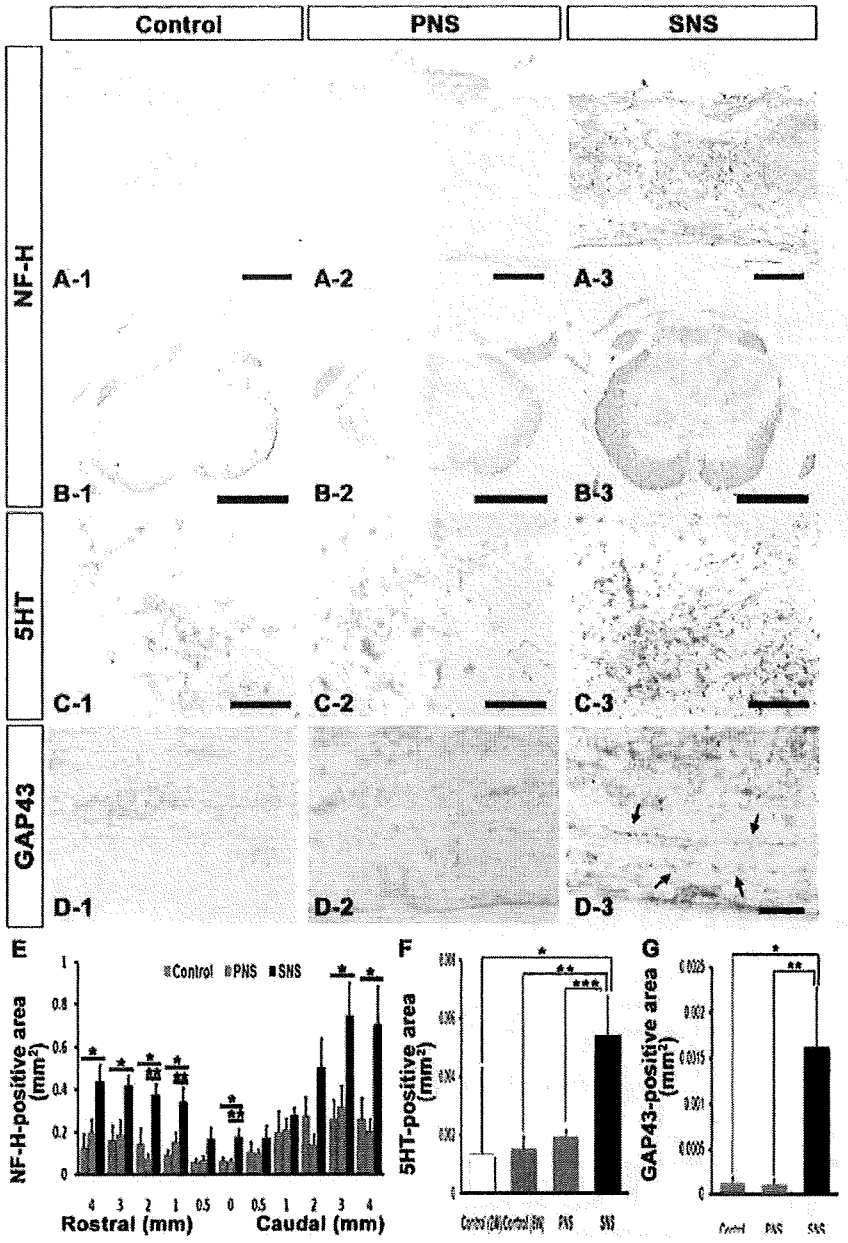

Figure 6. Transplanted SNS, but not PNS, promoted axonal growth. (A) Representative images of sagittal sections stained for NF-H in all three groups. Scale bar: 200 μm. (B) Representative images of axial sections stained for NF-H at the lesion epicenter in all three groups. Scale bar: 500 μm. (C) Representative images of axial sections stained for 5-HT 4 mm caudal to the epicenter from all three groups. Scale bar: 100 μm. (D) Representative images of midsagittal sections stained for GAP43 in the ventral region 1 mm caudal to the epicenter from all three groups, and intact spinal cord. Arrows: GAP43-positive fibers. Scale bar: 50 μm. (E) Quantitative analysis of the NF-H-positive area at each distance point. While few NF-H-positive neuronal fibers were observed at the rim of the lesion epicenter in both the control and PNS groups, there were significantly more NF-H-positive neuronal fibers in the SNS group (B-3) at the lesion epicenter, 1, 2, 3, 4 mm rostral and 3, 4 mm caudal to the lesion epicenter compared with the control group (B-1), and at the lesion epicenter and 1, 2 mm rostral to the lesion site compared with the PNS group (B-2). Values are means ± s.e.m. ($n=5$). *: $P<0.05$, Control vs. SNS. **: $P<0.05$, PNS vs. SNS. (F) Quantitative analysis of the 5-HT-positive area in axial sections 4 mm caudal to the lesion epicenter. Significantly more 5-HT-positive fibers were observed in the SNS group compared with the other groups. Values are means ± s.e.m. ($n=3$).*: $P<0.05$, Control (2 weeks after injury) vs. SNS. **: $P<0.05$, Control (6 weeks after injury) vs. SNS. ***: $P<0.05$, PNS vs. SNS. (G) Quantitative analysis of the GAP43-positive area in midsagittal sections in the ventral region 1 mm caudal to the epicenter. Significantly more GAP43-positive fibers were observed in the SNS group than in the other groups. Values are means ± s.e.m. ($n=4$). *: $P<0.05$, Control vs. SNS. **: $P<0.05$, PNS vs. SNS.

doi:10.1371/journal.pone.0007706.g006

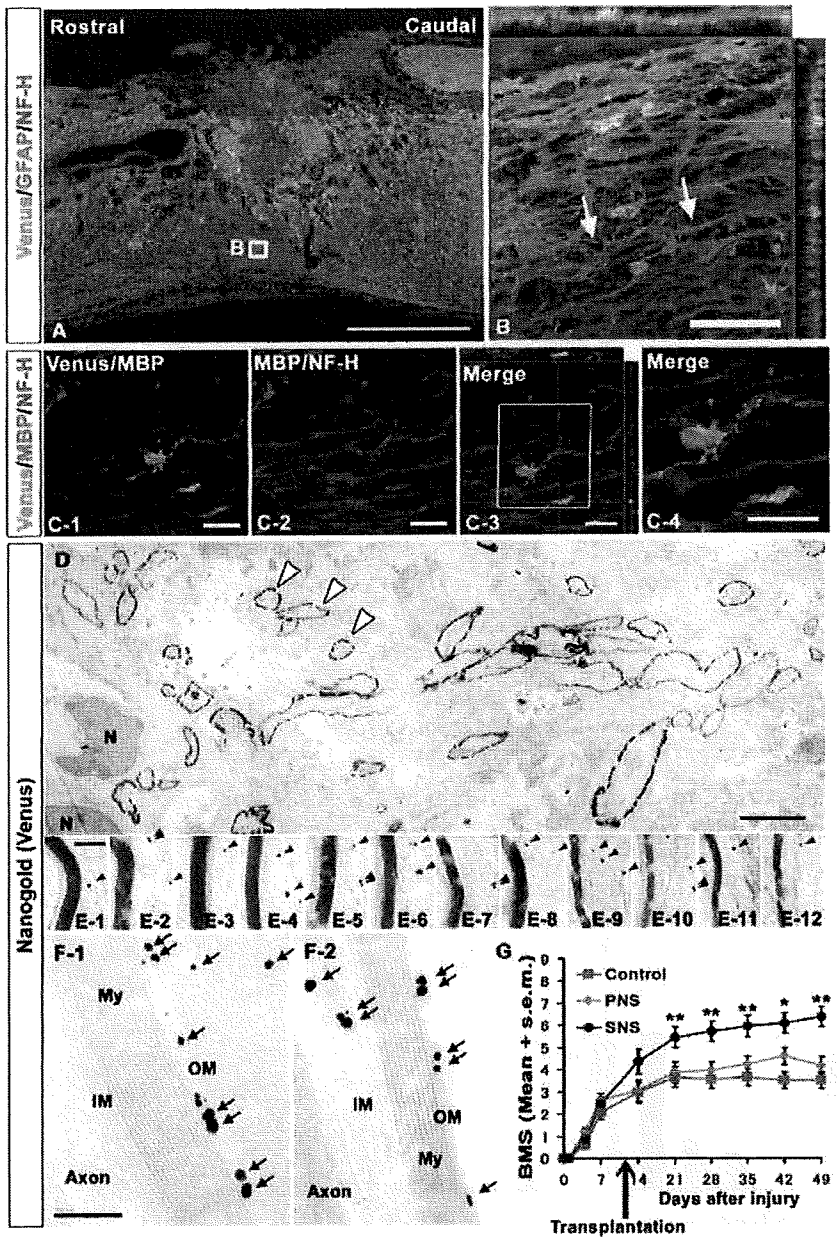

Figure 7. Transplanted SNS, but not PNS, promoted axonal growth, remyelination and functional recovery. (A) NF-H-positive neuronal fibers were observed along with GFAP-positive immature astrocytes derived either from the Venus-positive grafts or the host, and crossed the perilesional area in the SNS group. Scale bar: 50 μm. (B) Higher magnification images of the boxed area in A. Arrows: some examples of axons associated with Venus (GFP)-positive astrocytes. (C) Immunohistochemical analysis of MBP and NF-H in the SNS-transplanted injured spinal cord. SNS-derived Venus-positive cells differentiated into MBP-positive oligodendrocytes, which myelinated NF-H-positive fibers. Scale bar: 20 μm. (D)(E)(F) Representative electron-microscopic images of a remyelination site in sagittal sections from injured spinal cords grafted with SNS, which were immunostained for Venus (grafted cells) using an anti-GFP antibody. Low-magnification images show a group of grafted cells with active remyelination (some indicated by open arrowheads) (D). High-magnification images from (E-1) to (E-12) were obtained from (D), and show various numbers of lamellae in the myelin sheath. The remyelinating transplanted cells were detected as black dots (arrowheads). Venus (GFP)-positive dots (arrows) were localized to the outer and inner mesaxons of the myelin cytoplasm (OM, IM) (F). My: Myelination, N: Nucleus, Scale bar: 5 μm for D, 200 nm for E and F. (G) Mean Basso Mouse Scale for Locomotion (BMS) scores for each group over the 49-day recovery period. Although there was no significant difference in the BMS scores among the control, PNS, and SNS groups on day 14, the SNS group exhibited significantly better functional recovery than the PNS and control groups on day 21 and thereafter. On the other hand, there was no significant difference in the BMS scores between the PNS and control groups. Values are means ± s.e.m. ($n=11$), *: $P<0.05$, SNS vs. control, 42 days after injury. **: SNS vs. PNS or SNS vs. control on day 21, 28, 35, and 49 after injury.

doi:10.1371/journal.pone.0007706.g007

expected to be applied in cell replacement therapies for SCI [22]. However, detailed investigations of the optimal cell sources for promoting recovery from SCI are lacking. We recently developed an ES cell culture system that recapitulates the temporal progression of NS/PCs from the FGF-responsive early neurogenic NS/PCs to the EGF-responsive late gliogenic NS/PCs, consistent with CNS development *in vivo* [10,23] (Fig. 1**G, H**). Taking advantage of this difference in differentiation tendency, here we examined the distinct effects of the neurogenic PNS and gliogenic SNS on recovery following SCI.

One of the mechanisms underlying this developmental stage-dependent gliogenic transition of NS/PCs is the epigenetic regulation of glial cell-specific genes. The gradual demethylation of CpGs around the Stat3 recognition sequence in the GFAP promoter is thought to be involved in the developmental stage-dependent increase in transcription of the GFAP gene and the acquisition of astrocytic differentiation potentials [24,25,26]. Interestingly, this process is also observed in our ES cell-derived neurosphere system, in which the proportion of unmethylated CpGs in this region gradually increases during the development of ES cells into secondary neurospheres [10]. This may explain why the *in vitro* differentiation potentials of both the PNS and SNS were preserved even after their transplantation into injured spinal cord, despite its gliogenic environment (Fig. 4**A–F**) [27]. Since there was no significant difference in the numbers of grafted PNS and SNS in the injured spinal cord 6 weeks after transplantation, the difference in the in vivo differentiation potentials of the grafted neurospheres was the critical factor influencing the functional recovery after SCI. More than 70% of the grafted SNS cells differentiated into GFAP-positive astrocytes or APC-positive oligodendrocytes, and the engraftment of these cells led to improved functional recovery (Fig. 4**F**). In contrast, engrafted PNS cells, which mainly differentiated into neurons, did not promote functional recovery.

Determining the exact mechanisms through which the transplanted SNS, or glial cells, improved the recovery of the traumatically injured CNS has been challenging. The engrafted SNS cells could promote a wide range of effects, and here we showed positive effects of their transplantation on tissue sparing, myelination, angiogenesis, and axonal regeneration compared with the control group, and on myelination, angiogenesis, and axonal regeneration compared with the PNS group. One possible explanation for the functional recovery observed in the SNS group is that the SNS-derived astrocytes provided axonal guidance cues. This idea is supported by previous studies in which glial progenitors or glial progenitor-derived astrocytes were engrafted [28,29,30,31]. Immature astrocytes purified from the postnatal CNS have been shown to promote extensive neurite growth from a variety of neurons [32,33].

Although the reactive astrocytes in glial scar tissue express proteoglycans that can inhibit axonal growth, and have been shown to play a major role in the formation of misaligned scar tissue at sites of injury [34,35,36,37,38], we and others have previously shown that reactive astrocytes also have pivotal roles in the repair of injured tissue and recovery of motor function in the subacute phase after SCI, by sealing off injured areas and preventing the further spread of damage. They also produce an array of neurotrophic and growth factors [39]. Moreover, some astrocytes in the host spinal cord acquire stem-cell properties after injury and hence represent a promising cell type for initiating repair [40]. In combination with host astrocytes, immature astrocytes generated by the grafted SNS may express axonal growth-supporting molecules such as laminin, fibronectin, nerve growth factor (NGF), neurotrophin-3 (NT-3), vasoactive intestinal polypeptide (VIP), and activity-dependent neurotrophic factor (ADNF) [41] with minimal expression of chondroitin sulfate proteoglycans (CSPGs) [42]. In addition, SNS transplantation 9 days after SCI, between the acute and chronic phases, is likely to prevent grafted cells from differentiating into glial scar-forming reactive astrocytes due to their minimal expression of cytokines [3,43] and instead generate immature astrocytes, which provide cues for axonal regeneration. In fact, our immunohistochemical analysis revealed NF-H-positive neuronal fibers aligned with GFAP-positive fibers within the lesion site of the SNS group, suggesting that the SNS transplants promoted the alignment of regenerating axons with the fibers of astrocytes, which in turn promoted axonal growth into and out of the SNS grafts (Fig. 7**A and B**). In addition, the 5-HT-raphespinal system of the spinal cord has been shown to represent axonal regeneration after spinal cord injury [16,17], and the apparent regeneration and/or sparing of host 5-HT-positive fibers elicited by the grafting of SNS may have contributed to the observed functional recovery, since these fibers were not observed in the control or PNS groups (Fig. 6**C and F**).

Another possible explanation for the functional improvement in the SNS group is the enhancement of angiogenesis, since angiogenesis is reported to promote endogenous repair and support axonal outgrowth after SCI [44]. Under hypoxic conditions, astrocytes express angiogenic growth factors, including VEGF [45,46]. We revealed that transplanted SNS, but not PNS, enhanced angiogenesis after SCI (Fig. 5**A–Z**). We observed many host astrocytes (Fig. 5**N–Q**), and a few SNS-graft-derived astrocytes that expressed VEGF (Fig. 5**R–X**), suggesting that the SNS transplants promoted VEGF expression in both the host- and graft-derived GFAP-positive astrocytes. The increase in blood vessels elicited by the transplantation of ES cell-derived gliogenic NS/PCs may have improved axonal growth and prevented atrophy of the injured spinal cord.

The functional improvement might also be due to remyelination by SNS-derived oligodendrocytes, as supported by previous transplantation studies of ES cell-derived NS/PCs or oligodendrocyte progenitor cells (OPCs) [8,47]. While the neurogenic PNS dominantly differentiated into Hu-positive neurons (Fig. 4**F**), the gliogenic SNS differentiated into APC-positive oligodendrocytes that provided MBP-positive sheathes and promoted myelination after SCI (Fig. 2**C, D, F**, and Fig.7**C–F**).

In summary, here we took advantage of our recently established neurosphere-based culture system of ES cell-derived NS/PCs, in which PNS and SNS exhibit neurogenic and gliogenic potentials, respectively, and found that SNS cells were the most effective for promoting recovery after SCI. We showed that grafted SNS generated approximately equal numbers of GFAP-positive astrocytes and APC-positive oligodendrocytes in vivo. Both of these glial cell types may have contributed to the functional recovery, through trophic effects and the promotion of angiogenesis and axonal regeneration by immature astrocytes, and possibly through remyelination by grafted oligodendrocyte progenitor cells. Notably, the transplantation of PNS did not improve the functional recovery after SCI. These findings provide critical information for clinical trials using human ES- and induced pluripotent stem cell (iPS)-derived NS/PC transplantation for SCI.

Moreover, our results suggest that ES cell-derived NS/PCs cultured for relatively long periods may provide sufficient amounts of efficient glial donor cells for cell transplantation therapies. This strategy may also prevent the contamination of tumorigenic undifferentiated ES cells that occurs during long-term culture under serum-free conditions, and support the development of safe embryonic stem cell-based treatment strategies for spinal cord

injury. Although both the CCV-PNS- and CCV-SNS-derived Venus-positive cells survived without forming tumors for 6 weeks after transplantation in this study, careful observation for a longer period will be necessary to assess the possibility of tumor formation.

In the near future, other types of pluripotent stem cells, such as nuclear transfer ES (ntES) and iPS cells, which avoid the risk of immunological rejection and ethical concerns, will need to be evaluated to examine the applicability of human ES cells and human iPS cells in clinical applications.

Materials and Methods

ES Cell Culture and Differentiation

Mouse ES cells (EB3) [13] grown on gelatin-coated (0.1%) tissue-culture dishes were maintained in standard ES cell medium and used for EB formation as previously described, with slight modifications [9,13,48]. For neural induction, ES cells were dissociated into single cells with 0.25% trypsin-EDTA and cultured in bacteriological dishes for 6 days, to allow the formation of EBs. A low concentration of RA (low-RA; 10^{-8} M, Sigma) was added on day 2 of EB formation. The EBs were dissociated into single cells with 0.25% trypsin-EDTA and cultured in suspension at 5×10^4 cells/ml for 7 days in Media hormone mix (MHM) medium with 20 ng/ml FGF2 (Peprotech) and 2% B27 (Invitrogen), to obtain primary neurospheres (PNS). These PNS were dissociated into single cells with TripleLE Select (Invitrogen) and cultured again in suspension at 5×10^4 cells/ml for 7 days under the same conditions, to form secondary neurospheres (SNS) (Fig. 1**B**) [10]. For differentiation analysis, PNS and SNS were allowed to differentiate on poly-L-ornithine/fibronectin-coated coverslips for 5 days, followed by immunocytochemistry. The frequency of colonies consisting of βIII tubulin-positive neurons, GFAP-positive astrocytes, and O4-positive oligodendrocytes (N, A, O: colonies containing more than 20 positive cells are in capital letters; n, a, o: colonies containing fewer than 19 cells are in lower-case letters) is presented as the percentage of total colonies (50 colonies each) from three independent experiments.

Transfection of CAG-CBRluc-IRES-Venus

To visualize transplanted cells by both fluorescence and luminescence, we established an ES cell line that constitutively expresses a click beetle red-emitting luciferase variant (CBR*luc*) [11] and Venus [a yellow fluorescence protein (YFP) mutant] [12] by transfecting a linearized CAG-CBR*luc*-IRES-Venus plasmid (CCV; Fig. 1**A**) into EB3 ES cells using lipofectamine2000 (Invitrogen). Stably transfected ES cells were selected by G418 (200 μg/ml), subcloned, and screened by the expression of both CBR*luc* and Venus. The Venus could be detected by antibodies against EGFP.

Flow Cytometry

Undifferentiated ES cells, PNS, and SNS were dissociated and processed for flow cytometric analysis by FACS Calibur (Becton-Dickinson). The Venus-positive cells were counted and are presented as the percentage of the total number of cells, excluding dead cells stained by propidium iodide.

Spinal Cord Injury Model and Transplantation

Adult female C57BL/6J mice (20–22 g) were anesthetized via intraperitoneal (i.p.) injection of ketamine (100 mg/kg) and xylazine (10 mg/kg). After laminectomy at the 10th thoracic spinal vertebra (T10), a contusive SCI was induced at the same level using a commercially available SCI device (IH impactor, Precision Systems and Instrumentation, Lexington, KY), as described previously [49]. This device creates a reliable contusion injury by rapidly applying a force-defined impact (60 kdyn) with a stainless steel-tipped impounder. The initial touch point of the impactor with the dura was determined (using the vibrator mode of the impactor tip), and from there a 1.5-mm displacement was applied to the spinal cord. Force curve readings revealed an average value of 63±0.5 kdyn.

Nine days after the injury, CCV-PNS (n = 11) or -SNS (n = 11) that had been cultured for 7 days were partially dissociated and transplanted into the lesion epicenter using a glass micropipette (5×10^5 cells/mouse) and stereotaxic injector (KDS 310, Muromachi-kikai, Tokyo, Japan). An equal volume of PBS was injected into the control group (n = 11). Hind limb motor function was evaluated for 6 weeks after SCI using the locomotor rating test of the Basso-Mouse-Scale (BMS), as described previously [21]. Well-trained investigators, blinded to the treatments, performed the behavioral analysis, determining the BMS scores at the same time each day. All animal experiments were approved by the ethics committee of Keio University, and were in accordance with the Guide for the Care and Use of Laboratory Animals (National Institutes of Health, Bethesda, MD).

Bioluminescence Imaging (BLI)

BLI was performed using a Xenogen-IVIS 100 cooled CCD optical macroscopic imaging system (SC BioScience, Tokyo, Japan) [3,50]. To examine the effective expression of CBR*luc in vitro*, we used a CCD-based macroscope detector to determine the luminescence intensity of cultures with various numbers of cells (0 to 5×10^5 cells per well) in the presence of D-luciferin (150 μg/ml). The integration time was fixed at a 5-min duration for each image, and the signals were reported as photons/cells/sec. For *in vivo* BLI, D-luciferin was injected i.p. into mice (150 mg/kg body weight), and serial images were acquired 15–40 min. later, until a maximum signal intensity was obtained with the field-of-view, which was set at 15 cm. We found this time window to be optimal, since the signal intensity peaked 15–40 min after D-luciferin administration, and was followed by a 15-min plateau (data not shown). All images were analyzed with Igor (WaveMetrics, Lake Oswego, OR) and Living Image software (Xenogen, Alameda, CA), and the optical signal intensity was expressed as photon flux, in units of photons/sec/cm^2/steradian. The results were displayed as a pseudocolor photon count image superimposed on a grayscale anatomic image. To quantify the measured light, we defined a region of interest (ROI) over the cell-implanted area and examined all the values within the same ROI. The signal intensity of the engrafted cells was measured weekly for 6 weeks after transplantation.

Histological Analyses

Animals were anesthetized and transcardially perfused with 4% paraformaldehyde in 0.1 M PBS 6 weeks after transplantation. The spinal cords were removed, embedded in OCT compound (Sakura Finetechnical Co., Ltd.), and sectioned in the sagittal/axial plane at 20 μm on a cryostat (Leica CM3050 S). The injured spinal cords from the three groups were histologically evaluated by Hematoxylin-eosin (H-E) staining, Luxol Fast Blue (LFB) staining, and immunohistochemistry. The injured spinal cord from the vehicle control group 2 weeks after SCI was also evaluated by LFB staining and immunohistochemistry for 5-HT. Both cultured cells and tissue sections were stained with the following primary antibodies: anti-GFP (rabbit IgG, 1:500, MBL), anti-βIII tubulin (mouse IgG, 1:1000, Sigma), Alexa488-conjugated anti-βIII tubulin (mouse IgG, 1:4000, Covance), anti-Hu (human IgG,

1:1000, a gift from Dr. Robert Darnell, The Rockefeller University), anti-GFAP (rabbit IgG, 1:4000, Dako), anti-GFAP (guinea pig IgG, 1:4000, Advanced Immunochemical Inc.), anti-GFAP (rat IgG, 1:200, Invitrogen), anti-O4 (mouse IgM, 1:5000, Chemicon), anti-APC CC-1 (mouse IgG, 1:100, Calbiochem), anti-MBP (chicken IgY, 1:200, Aves Labs), anti-Neurofilament RT97 (NF-H, mouse IgG, 1:200, Chemicon), anti-5-HT (goat IgG, 1:200, Immunostar), anti-GAP43 (mouse IgG, 1:2000, Chemicon), Cy3-conjugated anti-SMA (mouse IgG 1:500, Sigma), anti-PECAM-1 (rat IgG, 1:50, BD Bioscience Pharmingen), and anti-VEGF (rabbit IgG, 1:50, Santa Cruz Biotechnology).

For immunohistochemistry with anti-Venus, VEGF, -NF-H, -5-HT, and -GAP43 antibodies, we used a biotinylated secondary antibody (Jackson Immunoresearch Laboratory, Inc.), after exposure to 0.3% H_2O_2 for 30 minutes at room temperature to inactivate endogenous peroxidase. The signals were enhanced with the Vectastain ABC kit (Vector Laboratories, Inc.). Nuclei were stained with Hoechst33258 (10 μg/ml, Sigma). The samples were examined with a universal fluorescence microscope (Axiocam, Carl Zeiss) or a confocal laser scanning microscope (LSM510, Carl Zeiss).

For immunoelectron microscopy, frozen sections were incubated with nanogold-conjugated anti-rabbit secondary antibody (1:100 Invitrogen) followed by incubation with the primary anti-GFP antibody. After enhancement with HQ-Silver kit (Nanoprobes Inc.), sections were postfixed with 0.5% osmium tetroxide, dehydrated through ethanol, and embedded in Epon. Ultrathin sections were stained with uranyl acetate and lead citrate, observed under a transmission EM (JEOL model 1230), and photographed with a Digital Micrograph 3.3 (Gatan Inc.).

Quantitative Analyses of Stained Tissue Sections through Transplanted Spinal Cord

To quantify HE-, LFB-, or immunostained sections, images were obtained by a universal fluorescence microscope (Axiocam, Carl Zeiss), manually outlined, and quantified by Micro Computer Imaging Device (MCID; Imaging Research Inc., St. Catharines, Ontario, Canada). Constant threshold values were maintained for all the analyses with MCID. HE-stained images were taken at the lesion epicenter and 2, 1, and 0.5 mm rostral and caudal to the epicenter in axial sections at ×25 magnification (n = 5, each). To analyze the LFB-positive area after transplantation, we automatically captured four regions from each animal in axial sections at the lesion epicenter and 2 mm and 1 mm rostral and caudal to the epicenter at ×200 magnification. Analyses were performed 2 weeks or 6 weeks after SCI for the vehicle-control group and 6 weeks after for the PNS and SNS groups. The total myelinated area was quantified by MCID using light intensity gain counting (n = 3, each). For the Venus (GFP)-positive area after transplantation, we captured in midsagittal sections the epicenter at ×25 magnification from each animal (6 weeks after SCI for the vehicle-control, PNS, and SNS groups), and quantified the total Venus-positive area (n = 6, each). NF-H-stained images were taken at the epicenter and 4, 3, 2, 1, and 0.5 mm rostral and caudal to the epicenter in axial sections at ×50 magnification, and the NF-H-positive areas were quantified using light intensity gain counting (n = 5, each). VEGF-stained images were taken at the lesion epicenter in axial sections at ×50, and the VEGF-positive areas were quantified using light intensity gain counting (n = 3, each). To analyze the 5-HT-positive area after transplantation, we automatically captured five regions from each animal in axial sections 4-mm caudal to the lesion epicenter (Th10 level), which was approximately at the L1 level, a non-lesion site, at ×200 magnification. The analysis was performed 2 weeks or 6 weeks after SCI for the vehicle-control group and 6 weeks after for the PNS and SNS groups. The total 5-HT-positive area was quantified (n = 3, for each condition). For the GAP43-positive area after transplantation, we captured the ventral regions in midsagittal sections 1 mm caudal to the epicenter at ×200 magnification from each animal (6 weeks after SCI for the vehicle-control, PNS, and SNS groups), and quantified the total GAP43-positive area (n = 4). To quantify the proportion of cells positive for each cell type-specific marker *in vivo*, we selected representative midsagittal sections and automatically captured five regions within 500 μm rostral and caudal to the lesion epicenter at ×200. The engrafted cells in each section that were positive for both Venus and each cell type-specific marker were counted (n = 4). The PECAM-1-positive blood vessels were counted manually in axial sections of the lesion epicenter at ×200 magnification (n = 3, each).

Statistical Analysis

All data are presented as the mean ± s.e.m. An unpaired two-tailed Student's *t*-test was used for the BLI analyses and Venus-stained analysis, and *in vivo* differentiation assays. ANOVA followed by the Turkey-Kramer test for multiple comparisons among the three transplantation groups was used for the *in vivo* differentiation analysis and PECAM-1-, VEGF-, 5HT-, and GAP43-stained analysis. Repeated measures two-way ANOVA followed by the Turkey-Kramer test was used for HE-, LFB-, NF-H-stained and BMS analysis. Pearson's correlation coefficient was used for correlation of the results of BLI analysis and the quantification of Venus-positive area. In all statistical analyses, the significance was set at $P<0.05$.

Acknowledgments

We thank Drs. H. J. Okano, K. Ishii, W. Akamatsu, S. Ishii, K. Miura, T. Nagai, S. Miyao, and T. Harada for technical assistance and scientific discussion, and all the members of Dr. Okano's laboratory for encouragement and kind support. We thank Drs. Y. Ishibashi, E. Tsuda, T. Yokoyama, and A. Ono for encouragement and kind support. We also thank Dr. H. Niwa for the EB3 cells.

Author Contributions

Conceived and designed the experiments: GK YO YT MN HO. Performed the experiments: GK YO JY NN KK MM OT KF HK SS. Analyzed the data: GK MN. Contributed reagents/materials/analysis tools: GK YO SO SS YM ST MN HO. Wrote the paper: GK YO HK MN HO.

References

1. Ogawa Y, Sawamoto K, Miyata T, Miyao S, Watanabe M, et al. (2002) Transplantation of in vitro-expanded fetal neural progenitor cells results in neurogenesis and functional recovery after spinal cord contusion injury in adult rats. J Neurosci Res 69: 925–933.
2. Iwanami A, Kaneko S, Nakamura M, Kanemura Y, Mori H, et al. (2005) Transplantation of human neural stem cells for spinal cord injury in primates. J Neurosci Res 80: 182–190.
3. Okada S, Ishii K, Yamane J, Iwanami A, Ikegami T, et al. (2005) In vivo imaging of engrafted neural stem cells: its application in evaluating the optimal timing of transplantation for spinal cord injury. Fasob J 19: 1839–1841.
4. Hofstetter CP, Holmstrom NA, Lilja JA, Schweinhardt P, Hao J, et al. (2005) Allodynia limits the usefulness of intraspinal neural stem cell grafts; directed differentiation improves outcome. Nat Neurosci 8: 346–353.
5. Cummings BJ, Uchida N, Tamaki SJ, Salazar DL, Hooshmand M, et al. (2005) Human neural stem cells differentiate and promote locomotor recovery in spinal cord-injured mice. Proc Natl Acad Sci U S A 102: 14069–14074.
6. Bibel M, Richter J, Schrenk K, Tucker KL, Staiger V, et al. (2004) Differentiation of mouse embryonic stem cells into a defined neuronal lineage. Nat Neurosci 7: 1003–1009.

7. McDonald JW, Liu XZ, Qu Y, Liu S, Mickey SK, et al. (1999) Transplanted embryonic stem cells survive, differentiate and promote recovery in injured rat spinal cord. Nat Med 5: 1410–1412.
8. Keirstead HS, Nistor G, Bernal G, Totoiu M, Cloutier F, et al. (2005) Human embryonic stem cell-derived oligodendrocyte progenitor cell transplants remyelinate and restore locomotion after spinal cord injury. J Neurosci 25: 4694–4705.
9. Okada Y, Shimazaki T, Sobue G, Okano H (2004) Retinoic-acid-concentration-dependent acquisition of neural cell identity during in vitro differentiation of mouse embryonic stem cells. Dev Biol 275: 124–142.
10. Okada Y, Matsumoto A, Shimazaki T, Enoki R, Koizumi A, et al. (2008) Spatio-Temporal Recapitulation of Central Nervous System Development By Murine ES Cell-Derived Neural Stem/Progenitor Cells. Stem Cells.
11. Zhao H, Doyle TC, Coquoz O, Kalish F, Rice BW, et al. (2005) Emission spectra of bioluminescent reporters and interaction with mammalian tissue determine the sensitivity of detection in vivo. J Biomed Opt 10: 41210.
12. Nagai T, Ibata K, Park ES, Kubota M, Mikoshiba K, et al. (2002) A variant of yellow fluorescent protein with fast and efficient maturation for cell-biological applications. Nat Biotechnol 20: 87–90.
13. Niwa H, Miyazaki J, Smith AG (2000) Quantitative expression of Oct-3/4 defines differentiation, dedifferentiation or self-renewal of ES cells. Nat Genet 24: 372–376.
14. Wang X, Rosol M, Ge S, Peterson D, McNamara G, et al. (2003) Dynamic tracking of human hematopoietic stem cell engraftment using in vivo bioluminescence imaging. Blood 102: 3478–3482.
15. Contag CH, Bachmann MH (2002) Advances in in vivo bioluminescence imaging of gene expression. Annu Rev Biomed Eng 4: 235–260.
16. Bregman BS (1987) Spinal cord transplants permit the growth of serotonergic axons across the site of neonatal spinal cord transection. Brain Res 431: 265–279.
17. Saruhashi Y, Young W, Perkins R (1996) The recovery of 5-HT immunoreactivity in lumbosacral spinal cord and locomotor function after thoracic hemisection. Exp Neurol 139: 203–213.
18. Ramon-Cueto A, Plant GW, Avila J, Bunge MB (1998) Long-distance axonal regeneration in the transected adult rat spinal cord is promoted by olfactory ensheathing glia transplants. J Neurosci 18: 3803–3815.
19. Kaneko S, Iwanami A, Nakamura M, Kishino A, Kikuchi K, et al. (2006) A selective Sema3A inhibitor enhances regenerative responses and functional recovery of the injured spinal cord. Nat Med 12: 1380–1389.
20. Kobayashi NR, Fan DP, Giehl KM, Bedard AM, Wiegand SJ, et al. (1997) BDNF and NT-4/5 prevent atrophy of rat rubrospinal neurons after cervical axotomy, stimulate GAP-43 and Talpha1-tubulin mRNA expression, and promote axonal regeneration. J Neurosci 17: 9583–9595.
21. Basso DM, Fisher LC, Anderson AJ, Jakeman LB, McTigue DM, et al. (2006) Basso Mouse Scale for locomotion detects differences in recovery after spinal cord injury in five common mouse strains. J Neurotrauma 23: 635–659.
22. Coutts M, Keirstead HS (2007) Stem cells for the treatment of spinal cord injury. Exp Neurol.
23. Temple S (2001) The development of neural stem cells. Nature 414: 112–117.
24. Fan G, Martinowich K, Chin MH, He F, Fouse SD, et al. (2005) DNA methylation controls the timing of astrogliogenesis through regulation of JAK-STAT signaling. Development 132: 3345–3356.
25. Shimozaki K, Namihira M, Nakashima K, Taga T (2005) Stage- and site-specific DNA demethylation during neural cell development from embryonic stem cells. J Neurochem 93: 432–439.
26. Takizawa T, Nakashima K, Namihira M, Ochiai W, Uemura A, et al. (2001) DNA methylation is a critical cell-intrinsic determinant of astrocyte differentiation in the fetal brain. Dev Cell 1: 749–758.
27. Winkler C, Fricker RA, Gates MA, Olsson M, Hammang JP, et al. (1998) Incorporation and glial differentiation of mouse EGF-responsive neural progenitor cells after transplantation into the embryonic rat brain. Mol Cell Neurosci 11: 99–116.
28. Hofstetter CP, Schwarz EJ, Hess D, Widenfalk J, El Manira A, et al. (2002) Marrow stromal cells form guiding strands in the injured spinal cord and promote recovery. Proc Natl Acad Sci U S A 99: 2199–2204.
29. Hill CE, Proschel C, Noble M, Mayer-Proschel M, Gensel JC, et al. (2004) Acute transplantation of glial-restricted precursor cells into spinal cord contusion injuries: survival, differentiation, and effects on lesion environment and axonal regeneration. Exp Neurol 190: 289–310.
30. Cao Q, Xu XM, Devries WH, Enzmann GU, Ping P, et al. (2005) Functional recovery in traumatic spinal cord injury after transplantation of multineurotrophin-expressing glial-restricted precursor cells. J Neurosci 25: 6947–6957.
31. Davies JE, Huang C, Proschel C, Noble M, Mayer-Proschel M, et al. (2006) Astrocytes derived from glial-restricted precursors promote spinal cord repair. J Biol 5: 7.
32. Baehr M, Bunge RP (1990) Growth of adult rat retinal ganglion cell neurites on astrocytes. Glia 3: 293–300.
33. Noble M, Fok-Seang J, Cohen J (1984) Glia are a unique substrate for the in vitro growth of central nervous system neurons. J Neurosci 4: 1892–1903.
34. Tang X, Davies JE, Davies SJ (2003) Changes in distribution, cell associations, and protein expression levels of NG2, neurocan, phosphacan, brevican, versican V2, and tenascin-C during acute to chronic maturation of spinal cord scar tissue. J Neurosci Res 71: 427–444.
35. Bundesen LQ, Scheel TA, Bregman BS, Kromer LF (2003) Ephrin-B2 and EphB2 regulation of astrocyte-meningeal fibroblast interactions in response to spinal cord lesions in adult rats. J Neurosci 23: 7789–7800.
36. De Winter F, Oudega M, Lankhorst AJ, Hamers FP, Blits B, et al. (2002) Injury-induced class 3 semaphorin expression in the rat spinal cord. Exp Neurol 175: 61–75.
37. Moreau-Fauvarque C, Kumanogoh A, Camand E, Jaillard C, Barbin G, et al. (2003) The transmembrane semaphorin Sema4D/CD100, an inhibitor of axonal growth, is expressed on oligodendrocytes and upregulated after CNS lesion. J Neurosci 23: 9229–9239.
38. Berry M, Maxwell WL, Logan A, Mathewson A, McConnell P, et al. (1983) Deposition of scar tissue in the central nervous system. Acta Neurochir Suppl (Wien) 32: 31–53.
39. Okada S, Nakamura M, Katoh H, Miyao T, Shimazaki T, et al. (2006) Conditional ablation of Stat3 or Socs3 discloses a dual role for reactive astrocytes after spinal cord injury. Nat Med 12: 829–834.
40. Buffo A, Rite I, Tripathi P, Lepier A, Colak D, et al. (2008) Origin and progeny of reactive gliosis: A source of multipotent cells in the injured brain. Proc Natl Acad Sci U S A 105: 3581–3586.
41. Blondel O, Collin C, McCarran WJ, Zhu S, Zamostiano R, et al. (2000) A glia-derived signal regulating neuronal differentiation. J Neurosci 20: 8012–8020.
42. Gallo V, Bertolotto A (1990) Extracellular matrix of cultured glial cells: selective expression of chondroitin 4-sulfate by type-2 astrocytes and their progenitors. Exp Cell Res 187: 211–223.
43. Nakamura M, Houghtling RA, MacArthur L, Bayer BM, Bregman BS (2003) Differences in cytokine gene expression profile between acute and secondary injury in adult rat spinal cord. Exp Neurol 184: 313–325.
44. Beattie MS, Bresnahan JC, Komon J, Tovar CA, Van Meter M, et al. (1997) Endogenous repair after spinal cord contusion injuries in the rat. Exp Neurol 148: 453–463.
45. Mense SM, Sengupta A, Zhou M, Lan C, Bentsman G, et al. (2006) Gene expression profiling reveals the profound upregulation of hypoxia-responsive genes in primary human astrocytes. Physiol Genomics 25: 435–449.
46. Yoshida H, Imaizumi T, Tanji K, Matsumiya T, Sakaki H, et al. (2002) Platelet-activating factor enhances the expression of vascular endothelial growth factor in normal human astrocytes. Brain Res 944: 65–72.
47. Liu S, Qu Y, Stewart TJ, Howard MJ, Chakrabortty S, et al. (2000) Embryonic stem cells differentiate into oligodendrocytes and myelinate in culture and after spinal cord transplantation. Proc Natl Acad Sci U S A 97: 6126–6131.
48. Hooper M, Hardy K, Handyside A, Hunter S, Monk M (1987) HPRT-deficient (Lesch-Nyhan) mouse embryos derived from germline colonization by cultured cells. Nature 326: 292–295.
49. Scheff SW, Rabchevsky AG, Fugaccia I, Main JA, Lumpp JE, Jr. (2003) Experimental modeling of spinal cord injury: characterization of a force-defined injury device. J Neurotrauma 20: 179–193.
50. Rice BW, Cable MD, Nelson MB (2001) In vivo imaging of light-emitting probes. J Biomed Opt 6: 432–440.

Journal of Neuroscience Research

Journal of Neuroscience Research 88:1394–1405 (2010)

Transplantation of Galectin-1-Expressing Human Neural Stem Cells Into the Injured Spinal Cord of Adult Common Marmosets

Junichi Yamane,[1,2] Masaya Nakamura,[2] Akio Iwanami,[1,2,3] Masanori Sakaguchi,[1] Hiroyuki Katoh,[2,3] Masayuki Yamada,[4,5] Suketaka Momoshima,[6] Sachiyo Miyao,[1,2] Ken Ishii,[2] Norikazu Tamaoki,[4] Tatsuji Nomura,[4] Hirotaka James Okano,[1] Yonehiro Kanemura,[7] Yoshiaki Toyama,[2] and Hideyuki Okano[1]*

[1]Department of Physiology, Keio University School of Medicine, Shinjuku, Tokyo, Japan
[2]Department of Orthopedic Surgery, Keio University School of Medicine, Shinjuku, Tokyo, Japan
[3]Research Division, National Organization, Murayama Medical Center, Tokyo, Japan
[4]Central Institute for Experimental Animals, Kawasaki, Kanagawa, Japan
[5]Faculty of Radiological Technology, Fujita Health University School of Health Sciences, Aichi, Japan
[6]Department of Radiology, Keio University School of Medicine, Shinjuku, Tokyo, Japan
[7]Institute for Clinical Research, Osaka National Hospital, National Hospital Organization, Osaka, Japan

Delayed transplantation of neural stem/progenitor cells (NS/PCs) into the injured spinal cord can promote functional recovery in adult rats and monkeys. To enhance the functional recovery after NS/PC transplantation, we focused on galectin-1, a carbohydrate-binding protein with pleiotropic roles in cell growth, differentiation, apoptosis, and neurite outgrowth. Here, to determine the combined therapeutic effect of NS/PC transplantation and galectin-1 on spinal cord injury (SCI), human NS/PCs were transfected by lentivirus with galectin-1 and green fluorescent protein (GFP), (Gal-NS/PCs) or GFP alone (GFP-NS/PCs), expanded in vitro, and then transplanted into the spinal cord of adult common marmosets, 9 days after contusive cervical SCI. The animals' motor function was evaluated by their spontaneous motor activity, bar grip power, and performance on a treadmill test. Histological analyses revealed that the grafted human NS/PCs survived and differentiated into neurons, astrocytes, and oligodendrocytes. There were significant differences in the myelinated area, corticospinal fibers, and serotonergic fibers among the Gal-NS/PC, GFP-NS/PC, vehicle-control, and sham-operated groups. The Gal-NS/PC-grafted animals showed a better performance on all the behavioral tests compared with the other groups. These findings suggest that Gal-NS/PCs have better therapeutic potential than NS/PCs for SCI in nonhuman primates and that human Gal-NS/PC transplantation might be a feasible treatment for human SCI. © 2010 Wiley-Liss, Inc.

Key words: spinal cord injury; galectin-1; common marmoset; neural stem/progenitor cells; preclinical study

It has long been believed that the adult mammalian central nervous system (CNS) does not regenerate after injury. In particular, spinal cord injury (SCI) has been intractable to neural regeneration and functional recovery (Horner and Gage, 2000; Okano, 2002a,b), owing to, among other factors, the limited ability of the CNS to replace lost cells (Johansson et al., 1999), axonal growth inhibitors associated with CNS myelin, fibrous and glial scars (Olson, 2002; David and Lacroix, 2003), and insufficient trophic support (Widenfalk et al., 2001). With recent progress in stem cell biology, however, several types of cells have become potential transplantation candidates for treating SCI, including embryonic stem (ES) cell-derived cells (McDonald et al., 1999; Keirstead et al., 2005), mesenchymal stem cells (MSCs; Hofstetter et al., 2002), olfactory ensheathing cells (OECs; Li et al., 1997), nestin-expressing multipotent hair follicle stem cells (Li et al., 2003; Amoh et al., 2008), and neural

Contract grant sponsor: Project to Realize Regenerative Medicine from the Japanese Ministry of Education, Sports and Culture; Human Frontier Science Program Organization; Contract grant sponsor: Core Research for Evolutional Science and Technology (CREST) from the Japan Science and Technology Corporation (JST); Contract grant sponsor: General Insurance Association of Japan; Contract grant sponsor: National Grant-in-Aid for the Establishment of a High-Tech Research Center in a Private University in Japan; Contract grant sponsor: Keio University Special Grant-in-Aid for Innovative Collaborative Research Projects (to H.O.); Contract grant sponsor: Grant-in-Aid from the Global COE Program of the Ministry of Education, Culture, Sports, Science and Technology, Japan (to Keio University); Contract grant sponsor: Keio University Grant-in-Aid for the Encouragement of Young Medical Scientists (to J.Y.).

*Correspondence to: Hideyuki Okano, Department of Physiology, Keio University School of Medicine, 35 Shinanomachi, Shinjuku, Tokyo, 160-8582, Japan. E-mail: hidokano@sc.itc.keio.ac.jp

Received 8 August 2009; Revised 3 October 2009; Accepted 19 October 2009

Published online 20 January 2010 in Wiley InterScience (www.interscience.wiley.com). DOI: 10.1002/jnr.22322

stem cells (NS/PCs; Cao et al., 2001; Ogawa et al., 2002).

To establish therapies involving NS/PC transplantation for SCI, we previously reported that the transplantation of rat NS/PCs promotes functional recovery after SCI in neonatal (Nakamura et al., 2005) and adult rats (Ogawa et al., 2002). We also established a graded SCI model in common marmosets (Iwanami et al., 2005b) and found that transplanted human NS/PCs promoted functional recovery after the injury in this model (Iwanami et al., 2005a). However, the observed functional recovery after NS/PC transplantation was not sufficient to qualify the procedure for a clinical trial in patients with complete SCI. Therefore, we have been seeking ways to enhance the functional recovery following NS/PC transplantation.

Lectins are carbohydrate-binding proteins with an affinity for β-galactoside-containing glycol conjugates. Galectin-1 (Gal-1) is a lectin observed in various normal and pathological tissues that appears to be functionally pleiotropic, with roles in a wide range of biological processes, including cell growth and differentiation, apoptosis, cell adhesion, tumor spreading, neurite outgrowth, and inflammation (Outenreath and Jones, 1992; Mahanthappa et al., 1994; Perillo et al., 1995, 1998; Puche et al., 1996; Rabinovich et al., 2000a,b, 2002). Previous reports demonstrated that Gal-1 is expressed on adult NS/PCs and promotes their proliferation through its carbohydrate-binding activity in the CNS (Sakaguchi et al., 2006). Furthermore, Gal-1 administration exhibited therapeutic effects against focal brain ischemia (Ishibashi et al., 2007) and also enhanced peripheral axonal regeneration (Horie et al., 1999). The purpose of the present study was to determine the effectiveness of transplanting human galectin-1-expressing human NS/PCs in promoting the recovery of motor functions in tetraplegic primates after contusive SCI.

MATERIALS AND METHODS

Tissue Samples and Neural Stem Cell Cultures

The ethical committees of Osaka National Hospital, the Tissue Engineering Research Center, and Keio University approved the use of human fetal neural tissues and neurosphere cultures. Tissue procurement was in accordance with the Declaration of Helsinki and in agreement with the ethical guidelines of the Network of European CNS Transplantation and Restoration (NECTAR) and the Japan Society of Obstetrics and Gynecology. Written informed consent was obtained from all the parents. By using the neurosphere culture method (Reynolds and Weiss, 1996; Nakamura et al., 2003), neural stem cells (NS/PCs) were cultured from the forebrain tissue of human fetuses (10 weeks gestational age) that were obtained through routine legal terminations performed at Osaka National Hospital.

Lentiviral Vector Expressing the h-Galectin-1 Gene

The third-generation self-inactivating HIV-1-based lentiviral vector, pCSII-EF-MCS-IRES2-Venus (Miyoshi et al., 1998), contained an internal ribosomal entry site (IRES); Venus, a variant of GFP (Nagai et al., 2002); and a woodchuck hepatitis virus post-transcriptional regulatory element (PRE). The h-galectin-1 gene fragment was excised from a human cDNA library and cloned into pCSII-EF-MCS-IRES2-Venus at the BamH1 site (Fig. 1A). Twenty-four hours before transfection, 293T cells were seeded in poly-L-lysine-coated T175 flasks. The cells were transfected using the lipofection protocol for the FuGENE6 transfection reagent (Roche, Indianapolis, IN). Two days after transfection, the conditioned medium was collected, and the virus was concentrated by centrifugation at 79,000*g* for 2 hr at 4°C. The pelleted virus was resuspended and stored at −80°C. The titer of the concentrated virus was approximately 5×10^8 transducing units per milliliter (TU/ml) when assayed using 293T cells, and infectivity was determined by the expression of GFP, which was analyzed by using a FACSCalibur (Becton-Dickinson, Franklin Lakes, NJ).

Lentiviral Transduction of Human NS/PCs

Human NS/PCs (hNS/PCs) that had undergone more than 10 passages by the neurosphere method were dissociated into single cells 2 hr before being infected. The concentrated viruses were then added to the culture medium to infect the hNS/PCs [multiplicity of infection (MOI) = 1.0]. Two weeks later, neurospheres were formed from the dissociated hNS/PCs (Fig. 1B) and were passaged as previously reported (Reynolds and Weiss, 1996; Nakamura et al., 2003). The efficiency of the transduction was measured by GFP expression with a FACSCalibur, as in the analysis of viral infectivity, and hNS/PCs with an efficiency of transduction greater than 80% were used for transplantation. Two types of lentivirus-transduced hNS/PCs were prepared: Gal-NS/PCs, hNS/PCs infected with the h-galectin-1 IRES Venus virus; and GFP-NS/PCs, hNS/PCs infected with the IRES Venus virus. Gal-NS/PCs, GFP-NS/PCs, and vehicle only were transplanted into the injured spinal cord. The expression of h-galectin-1 in all the hNS/PCs (Gal-NS/PCs, GFP-NS/PCs, and naive NS/PCs) was examined by Western blotting of cell lysates and conditioned media.

Proliferation Assay

The number of viable cells was indirectly analyzed by measuring ATP, a product of cell metabolism. After incubating the cultures in microplates at 37°C in 5% CO_2, 95% air for 24 hr or 144 hr, an ATP assay (CellTiter-GloTM Luminescent Cell Viability Assay; Promega, Madison, WI) was carried out according to the manufacturer's instructions. Briefly, 100 μl of Cell Titer-GloTM Reagent was added to each well, and the plate was incubated for 30 min at room temperature. The luminescent signal was detected using a chemiluminescence detection system (Wallac 1420 ARVOSX; Perkin-Elmer). The population doubling time (DT) was determined by using the ATP assay as described elsewhere (Kanemura et al., 2002).

Differentiation Assay

After the second passage, neurospheres prepared from Gal-NS/PCs, GFP-NS/PCs, or naive NS/PCs were dissociated into single cells and plated onto poly-L-lysine-coated

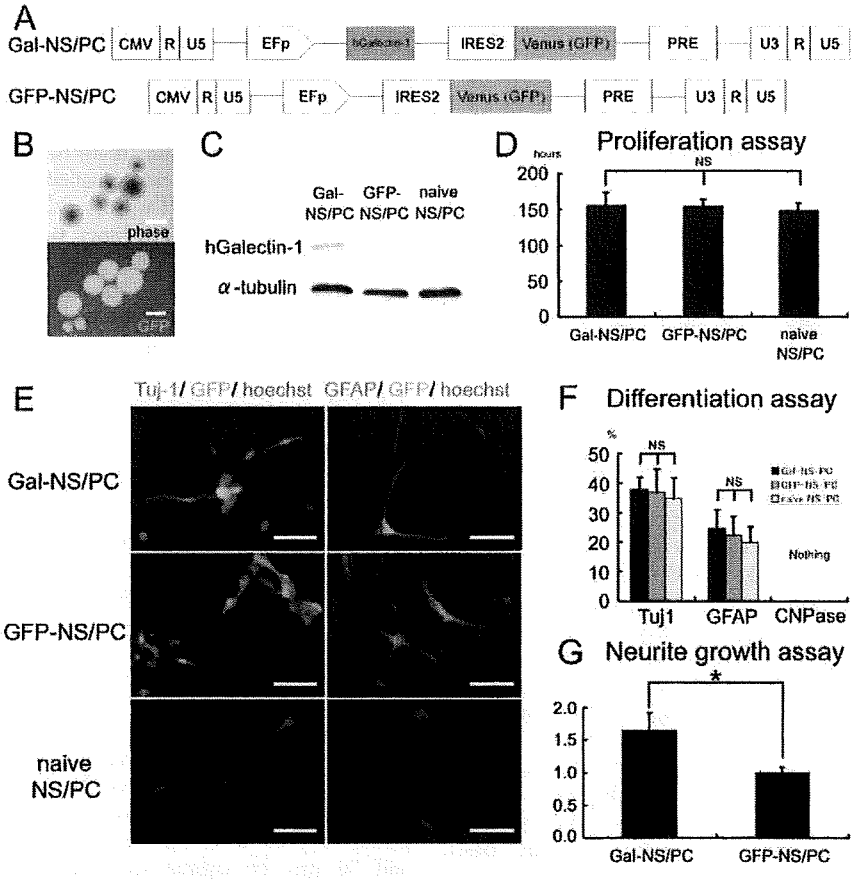

Fig. 1. Characterization of human NS/PCs in vitro. **A**: Lentiviral construct encoding a dual-function h-galectin-1 and GFP bicistronic reporter gene connected via an internal ribosomal entry site (IRES). **B**: Microscopic images of the lentivirally transduced human NS/PCs. **C**: Western blotting for h-galectin-1. A higher level of h-galectin-1 expression was observed in the Gal-NS/PCs. **D**: ATP assay. There was no significant difference in the proliferation rate among Gal-NS/PCs, GFP-NS/PCs, and naive NS/PCs. **E**: Differentiation assay. Lentiviral transfection did not influence the phenotype of human NS/PCs. Immunocytochemistry revealed that all of the human NS/PCs differentiated into Tuj1$^+$ neurons and GFAP$^+$ astrocytes, but not CNPase$^+$ oligodendrocytes (not shown), in vitro. **F**: Quantitative analyses of the differentiated phenotype of human NS/PCs. The proportions of the differentiated phenotypes in the lentivirally transduced NS/PCs (Gal-NS/PCs and GFP-NS/PCs) were identical to those of the untreated naive NS/PCs. **G**: Neurite growth assay. The neurites were significantly longer in the neurons derived from Gal-NS/PCs than in those derived from GFP-NS/PCs. The average length in GFP-NS/PCs was defined as 1.0. $*P < 0.05$. Scale bars = 100 μm in B; 50 μm in E.

coverslips at a density of 1×10^5 cells/ml in 10% FCS-containing medium. After 7 days in culture, the cells were fixed with 4% paraformaldehyde (PFA) in 0.1 M phosphate-buffered saline (PBS) for immunocytochemistry. Cultured cells were immunostained with the following primary antibodies: anti-GFP (1:500; MBL, Woburn, MA), anti-glial fibrillary acid protein (GFAP; 1:1,000; Dako, Glostrup, Denmark), anti-βIII tubulin (Tuj-1; 1:200; Sigma, St. Louis, MO), and anti-2′,3′-cyclic nucleotide 3′-phosphodiesterase (CNPase; 1:200; Sigma). Nuclei were counterstained with Hoechst 33342 (Molecular Probes, Eugene, OR). All images were obtained with a fluorescence microscope (Axioskop 2 plus; Carl Zeiss, Munich, Germany). After the differentiation assay, the neurite length of hNS/PCs that were double positive for GFP and βIII tubulin was measured by the MCID (microcomputer imaging device) system (Amersham Bioscience Corp., Piscataway, NJ). The neurite length of the Gal-NS/PCs relative to that of GFP-NS/PCs was determined.

Contusive SCI in Common Marmosets

Adult female common marmosets (*Callithrix jacchus*; Clea Japan Inc., Tokyo, Japan) were anesthetized with intramuscular injections of ketamine (50 mg/kg; Sankyo Co., Ltd., Tokyo, Japan) and xylazine (5 mg/kg; Bayer AG, Leverkusen, Germany) and by the inhalation of isofluren (Foren; Abbott Japan Co., Ltd., Tokyo, Japan). A moderate contusive SCI was induced in 21 marmosets using a modified NYU device, as previously reported (Iwanami et al., 2005b). In brief, a 17-g weight (3.5-mm in diameter) was dropped from a height of 50 mm onto the exposed dura mater at the C5 level. In the laminectomy group (n = 2), only a laminectomy was per-

formed. All the animals were placed in a temperature-controlled chamber until thermoregulation was reestablished. Micturition by manual bladder compression was performed twice per day until voiding reflexes were reestablished. Paralyzed animals were fed manually until they recovered their ability to ingest food and water without assistance. For 1 week after surgery, ampicillin (100 mg/kg; Meiji Seika Kaisha, Ltd., Tokyo, Japan) was injected intramuscularly into each animal. Prior approval of all animal procedures, which were in accordance with the NIH *Guide for the care and use of laboratory animals*, was obtained from the Keio University Ethics Committee and the Animal Experimentation Committee of the Central Institute for Experimental Animals.

Transplantation of hNS/PCs

hNS/PCs were transplanted into the injured spinal cord 9 days after the injury, at which time the microenvironment of the injured spinal cord changes from the inhospitable setting of the acute phase to one that supports the survival and differentiation of transplanted NS/PCs (Ogawa et al., 2002; Okano, 2002a; Nakamura et al., 2003; Okano et al., 2003). After the animals were again anesthetized, partially dissociated neurospheres at a density of approximately 1.0×10^6 cells/5 μl in medium without growth factors (Gal-NS/PCs or GFP-NS/PCs, n = 7) or a medium vehicle without growth factors (vehicle-control group, n = 7) were injected into the lesion epicenter using a glass pipette fitted to a 25-μl Hamilton syringe and a microstereotaxic injection system (David Kopf Instruments, Tujunga, CA). All the animals received daily ampicillin for 1 week after the transplantation and daily subcutaneous cyclosporine injections (10 mg/kg; Novartis, Basel, Switzerland) until they were sacrificed for analysis.

MRI

The magnitude of the SCI and the changes after injury were evaluated by magnetic resonance imaging (MRI), with which pathogenic events such as hemorrhage, edema, and cavity formation can be assessed in real time (Ohta et al., 1999; Metz et al., 2000). With a 7.0-Tesla superconducting imager (Bruker, Rheinstetten, Germany) fitted with a phased-array volume coil, MRI of the injured spinal cord was conducted 3 days after injury and 12 weeks after transplantation under the following conditions: 1) sagittal and 2) axial T2-weighted (T2W) fast spin-echo with a TR/TE number averaging 4,000 msec/100 msec/15, field-of-view of 9 cm, matrix of 256 × 256, and section thickness of 1.7 mm, and 3) sagittal T1-weighted (T1W) spin echo with a TR/TE number averaging 400 msec/12 msec/15 (all other parameters the same as given above).

Behavioral Analyses

The motor function of all the common marmosets was evaluated by measuring their spontaneous motor activity and bar grip power, as previously described (Iwanami et al., 2005b) and by introducing a treadmill test to assess higher locomotor function.

Measurement of spontaneous motor activity. Spontaneous motor activity is difficult to evaluate in common marmosets because of their three-dimensional movement (that is, they climb as well as walk around their enclosures). In the present study, we used cages (350-mm wide, 500-mm deep, 500-mm high) equipped with infrared sensors (Murata Manufacturing Corp., Nagaokakyo, Kyoto, Japan) on the ceiling and continually recorded the marmosets' motions in all three dimensions. The data were uploaded to a computer every hour, and the activity after SCI was quantified and expressed as a percentage of the animal's activity before the injury (Iwanami et al., 2005b).

Bar grip power. The motor function of the upper extremities was evaluated by a bar grip power test, which examines the animal's gripping reflex (the motion undertaken when attempting to grasp an object placed before the animal). The test was performed three times per day, and the maximal grip strength as a percentage of that before the injury was calculated (Iwanami et al., 2005b).

Treadmill test. The locomotive function of each marmoset was evaluated by using a treadmill test. The maximum velocity at which the animal could walk or run was recorded once per week, and the velocity after SCI as a percentage of that before the injury was calculated.

Histological Analyses

Thirteen weeks after transplantation, each animal was deeply anesthetized and intracardially perfused with 4% PFA (pH 7.4). The spinal cord tissues were removed, postfixed in 4% PFA, and immersed overnight in 10% sucrose followed by 30% sucrose. The cord was then embedded in OCT compound and sectioned on a cryostat at 20 μm for axial sections and 30 μm for sagittal sections. The sections were stained with hematoxylin-eosin (H-E) for general histological examinations and with Luxol fast blue (LFB) to evaluate the myelinated area after SCI. The area of myelinated fibers in axial sections of the lesion epicenter was measured using the MCID system and compared among the three (Gal-NS/PC, GFP-NS/PC, or vehicle-control) groups. To assess the corticospinal tract (CST), sections were immunostained with an anticalmodulin-dependent protein kinase II alpha (CaMKIIα) antibody (1:100; mouse monoclonal; Zymed, CA; secondary antibody was HRP-labeled goat anti-mouse IgG for TSA, ABC, and DAB staining), and the serotonergic fibers were immunostained with an anti-5HT antibody (1:100; rabbit polyclonal; Diasorin, Venice, Italy; secondary antibody was Alexa 568 goat anti-rabbit IgG; 1:500; Molecular Probes). The total areas positive for CaMKIIα or 5HT in axial sections of the lesion epicenter were measured using the MCID system and compared among the three groups.

The hNS/PCs grafted into the injured spinal cords were identified by using an anti-GFP antibody (1:200; MBL), and their phenotypes were examined by immunostaining for the following cell-type-specific markers: antiglutathione S-transferase pi (GSTpi; 1:500; mouse monoclonal; BD Biosciences, San Jose, CA), anti-Hu (Okano and Darnell, 1997; 1:200; a gift from R. Darnell, The Rockefeller University), and anti-GFAP (1:200; Dako, Glostrup, Denmark). To evaluate associations between the grafted cells and the host axons or myelin sheath around the lesion epicenter, triple immunostaining for